

核子多体系の基本的性質と 原子核集団運動

中務 孝

理研・仁科加速器研究センター

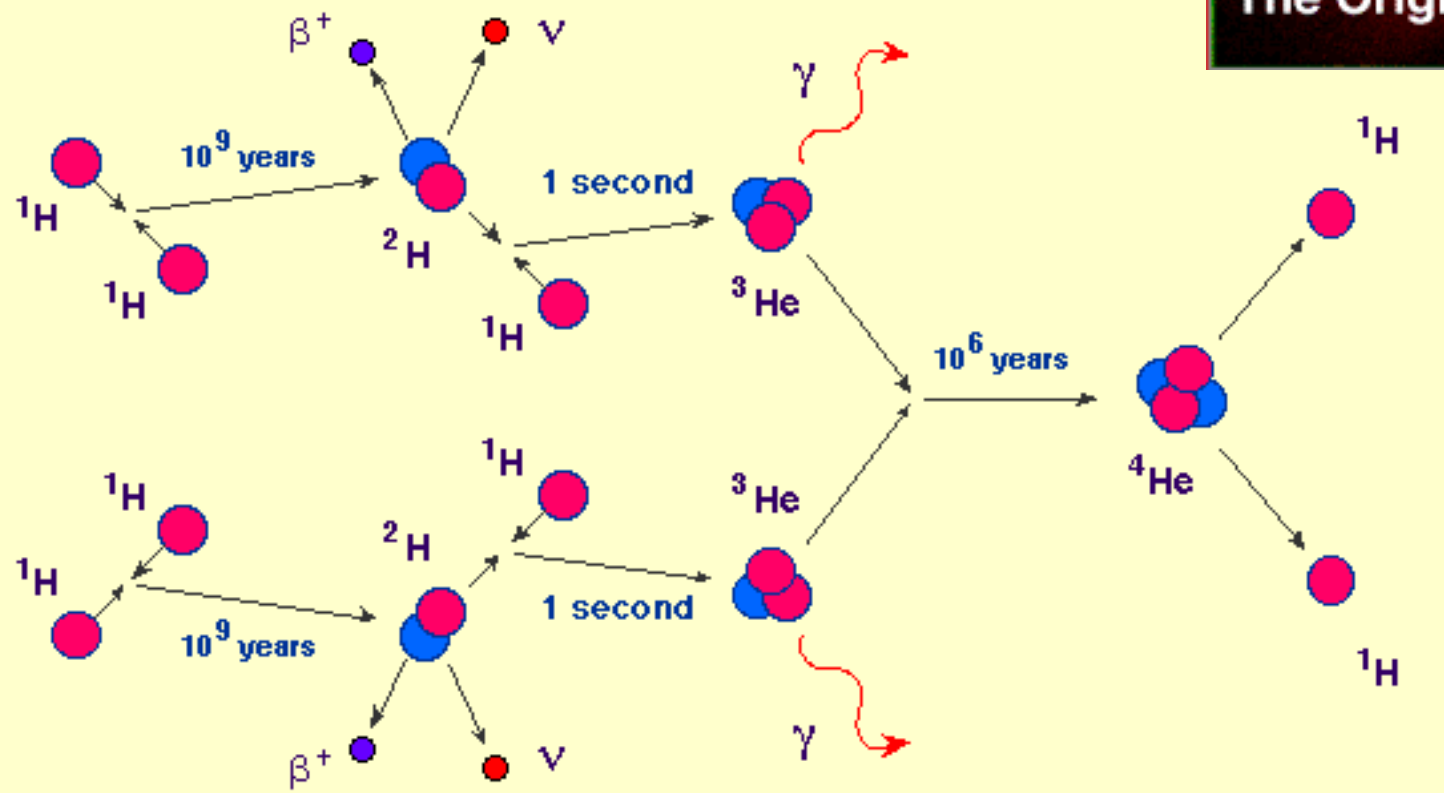
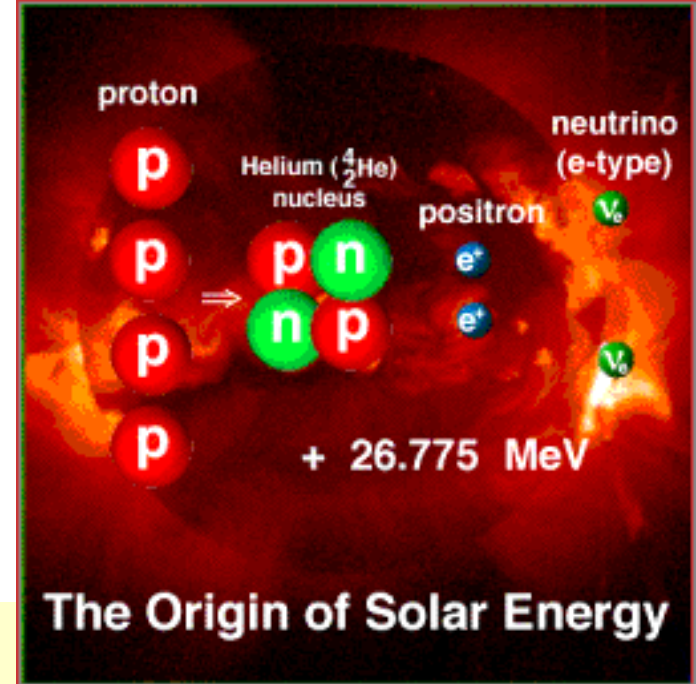
2013.12.25 中性子星核物質ウィンタースクール 講義

Contents

- Basic properties of nuclear systems
- Different aspects in different time scales
- Symmetry breaking in finite time scale
- Rapidly rotating nuclei
- Superdeformation and new type of symmetry breaking

ppチェイン

- $p(p,e^+\nu)d$ reaction determines the lifetime of the sun



核物理に関する異なる反応率

- 移行反応 (強い相互作用)

- $^{15}\text{N}(p,\alpha)^{12}\text{C}$ $1 \text{ b} = 100 \text{ fm}^2$

- $\sigma \sim 0.5 \text{ b}$ ($E=2 \text{ MeV}$)

- 捕獲反応 (電磁気相互作用)

- $^3\text{He}(\alpha,\gamma)^7\text{Be}$

- $\sigma \sim 10^{-6} \text{ b}$ ($E=2 \text{ MeV}$)

- 弱過程 (弱い相互作用)

- $p(p,\text{e}^+\nu)d$

- $\sigma \sim 10^{-20} \text{ b}$ ($E=2 \text{ MeV}$)



異なる時間スケール



液滴模型

束縛エネルギー

$$B/A \approx 8 \text{ MeV}$$

密度分布

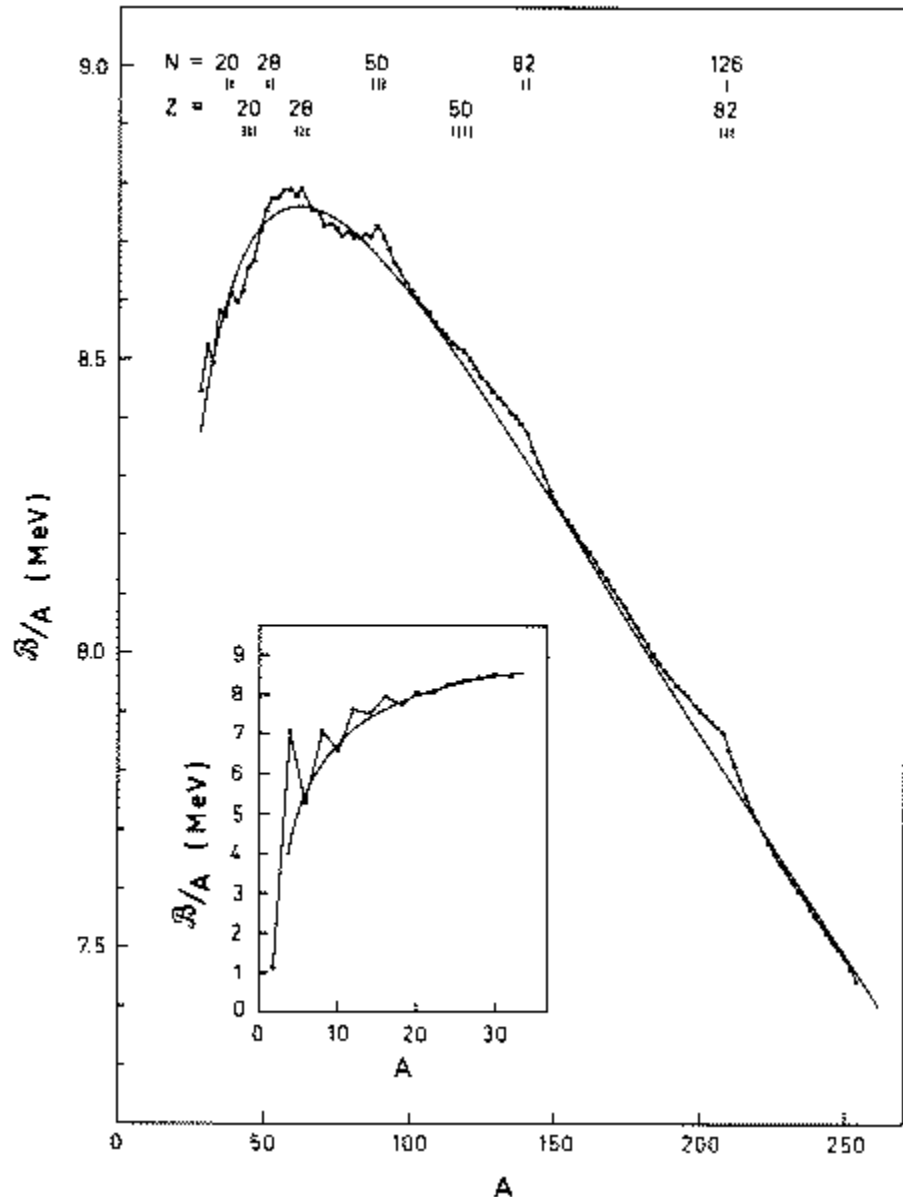
$$\rho \approx 0.16 \text{ fm}^{-3} \quad d \approx 2 \text{ fm}$$

飽和性 (Saturation)

Bethe-Weizsäcker 質量公式

$$B(N, Z) = a_V A - a_S A^{2/3} - a_{sym} \frac{(N - Z)^2}{A} - a_C \frac{Z^2}{A^{1/3}} + \delta(A)$$

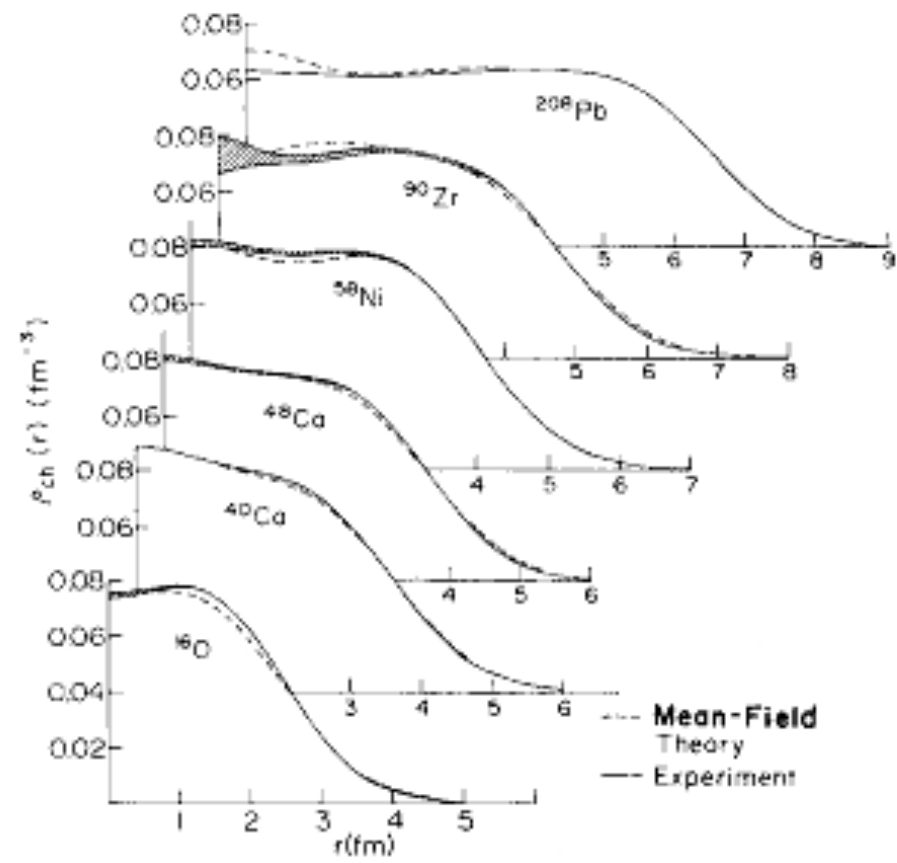
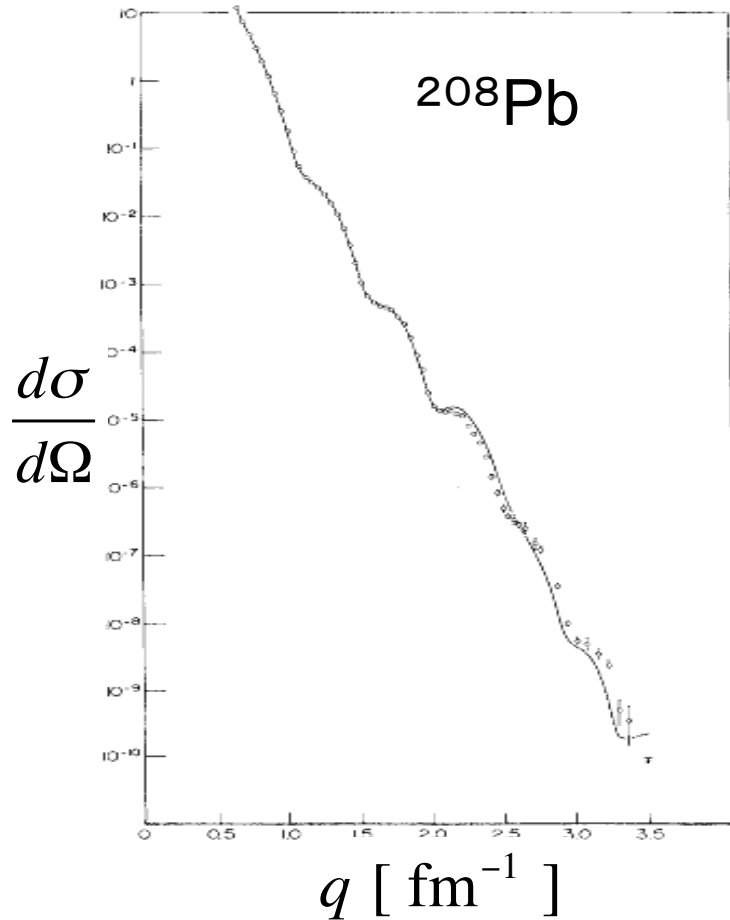
Bohr & Mottelson
Nuclear Structure Vol. 1



原子核の電子散乱

- 原子核の電子散乱

$$\rho(\vec{r}) = \frac{1}{(2\pi)^3} \int G_E(q^2) e^{-i\vec{q}\cdot\vec{r}} d\vec{q}$$



Mayer-Jensen's Shell Model

調和振動子ポテンシャル + スピン・軌道ポテンシャル

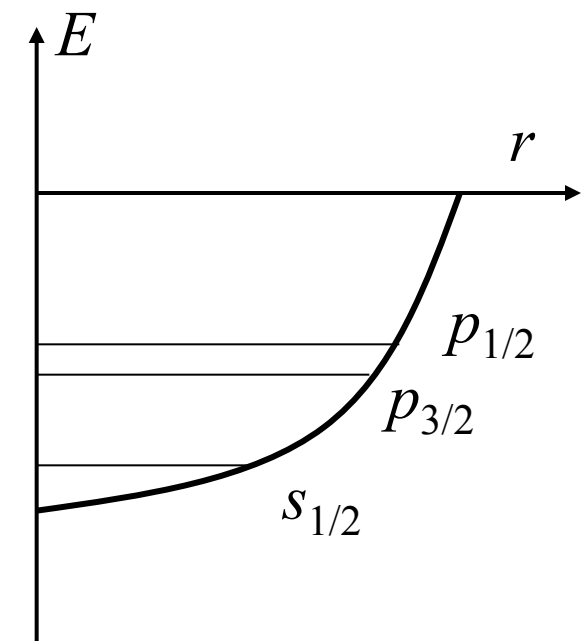
$$V(r) = \frac{1}{2} M \omega^2 r^2 + \nu_{ll} \ell^2 + \nu_{ls} \vec{\ell} \cdot \vec{s}$$

→ 魔法数(magic numbers):

(N,Z)=2, 8, 20, 28, 50, 82, 126

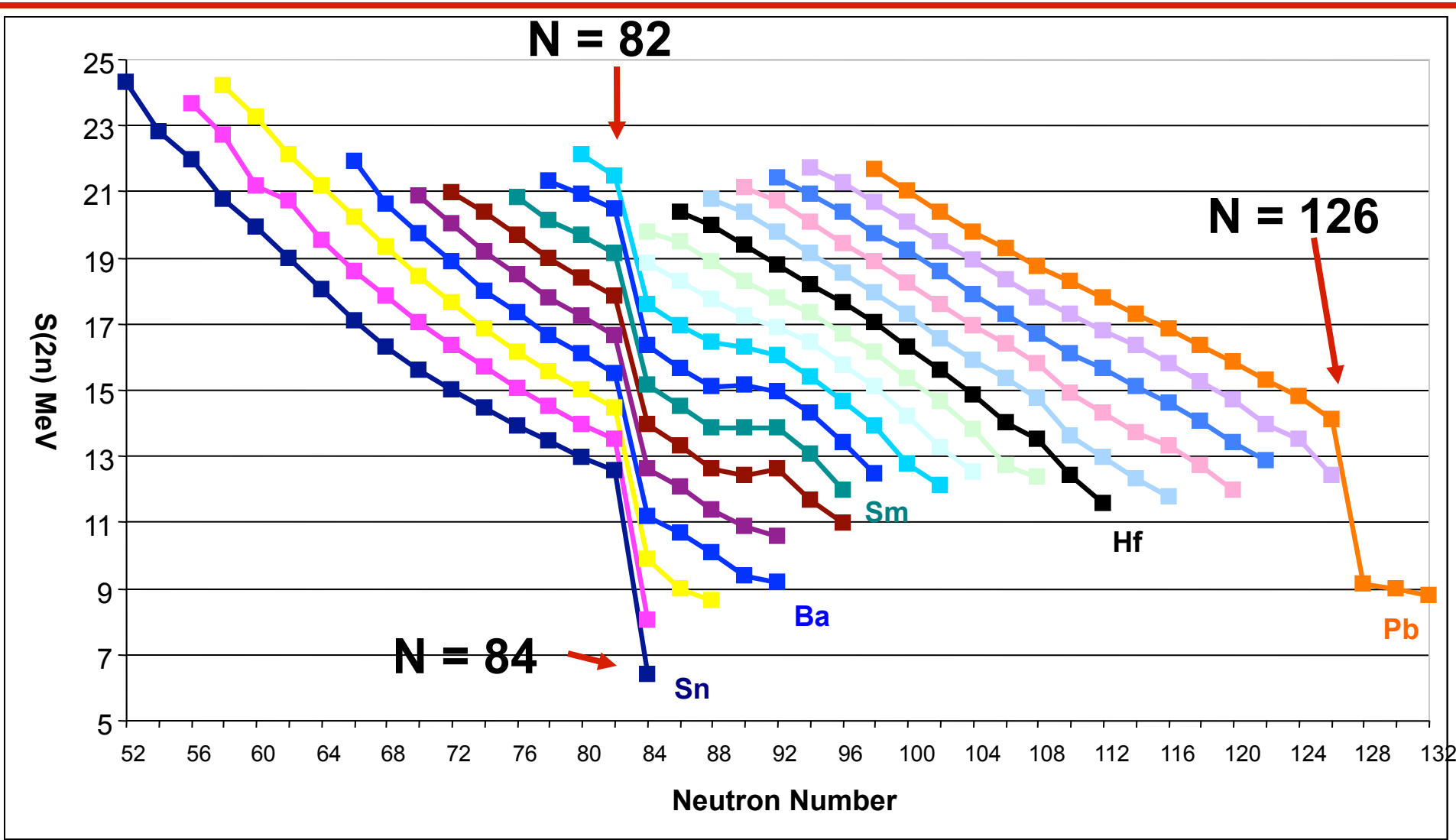
“气体”的な性質

$$\lambda \gg R$$

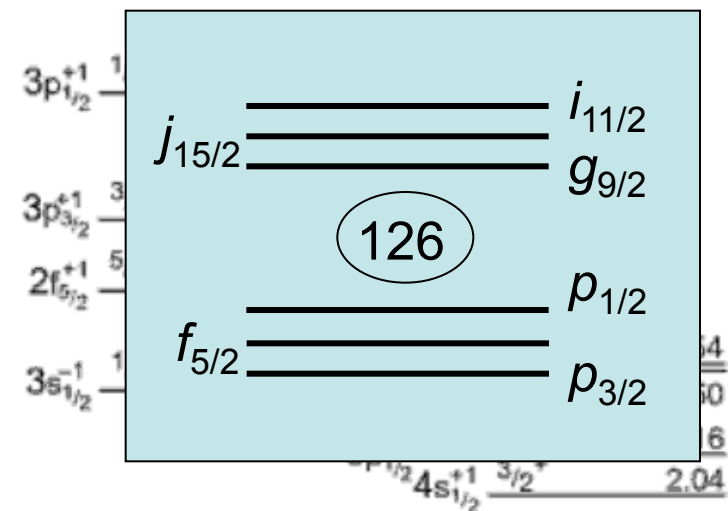
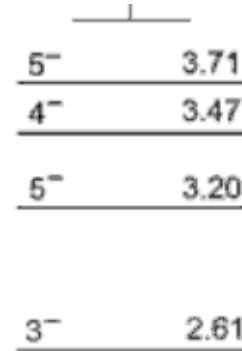
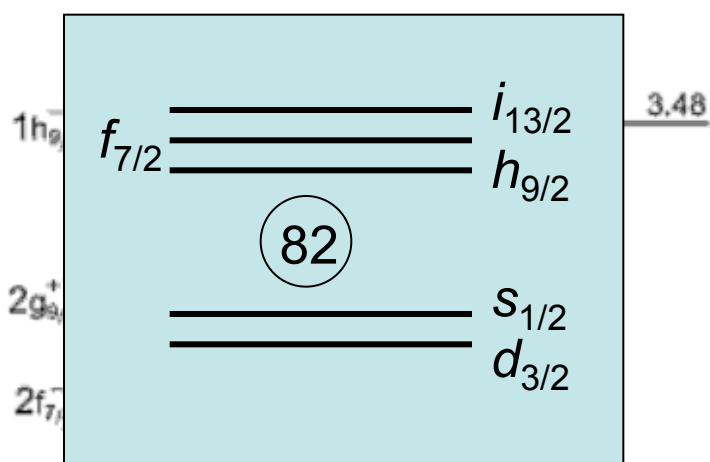


平均自由行程は原子核の大きさよりもはるかに大きい

2中性子分離エネルギー (= 2中性子束縛エネルギー)



Spin-parity of odd nuclei



$$1i_{13/2}^{-1} \frac{13/2^+}{1.63} \quad 2d_{5/2}^{-1} \frac{5/2^+}{1.67}$$

$$1h_{11/2}^{-1} \frac{11/2^-}{1.34}$$

$$3p_{3/2}^{-1} \frac{3/2^-}{0.90}$$

$$2f_{5/2}^{-1} \frac{5/2^-}{0.57}$$

$$2d_{3/2}^{-1} \frac{3/2^+}{0.35}$$

$$3p_{1/2}^{-1} \frac{1/2^-}{0.00}$$

$$3s_{1/2}^{-1} \frac{1/2^+}{0.00}$$

$^{207}_{82}\text{Pb}_{125}$

$^{207}_{81}\text{Tl}_{126}$

$$1i_{13/2}^{+1} \frac{13/2^+}{1.61} \quad 3d_{5/2}^{+1} \frac{5/2^+}{1.57}$$

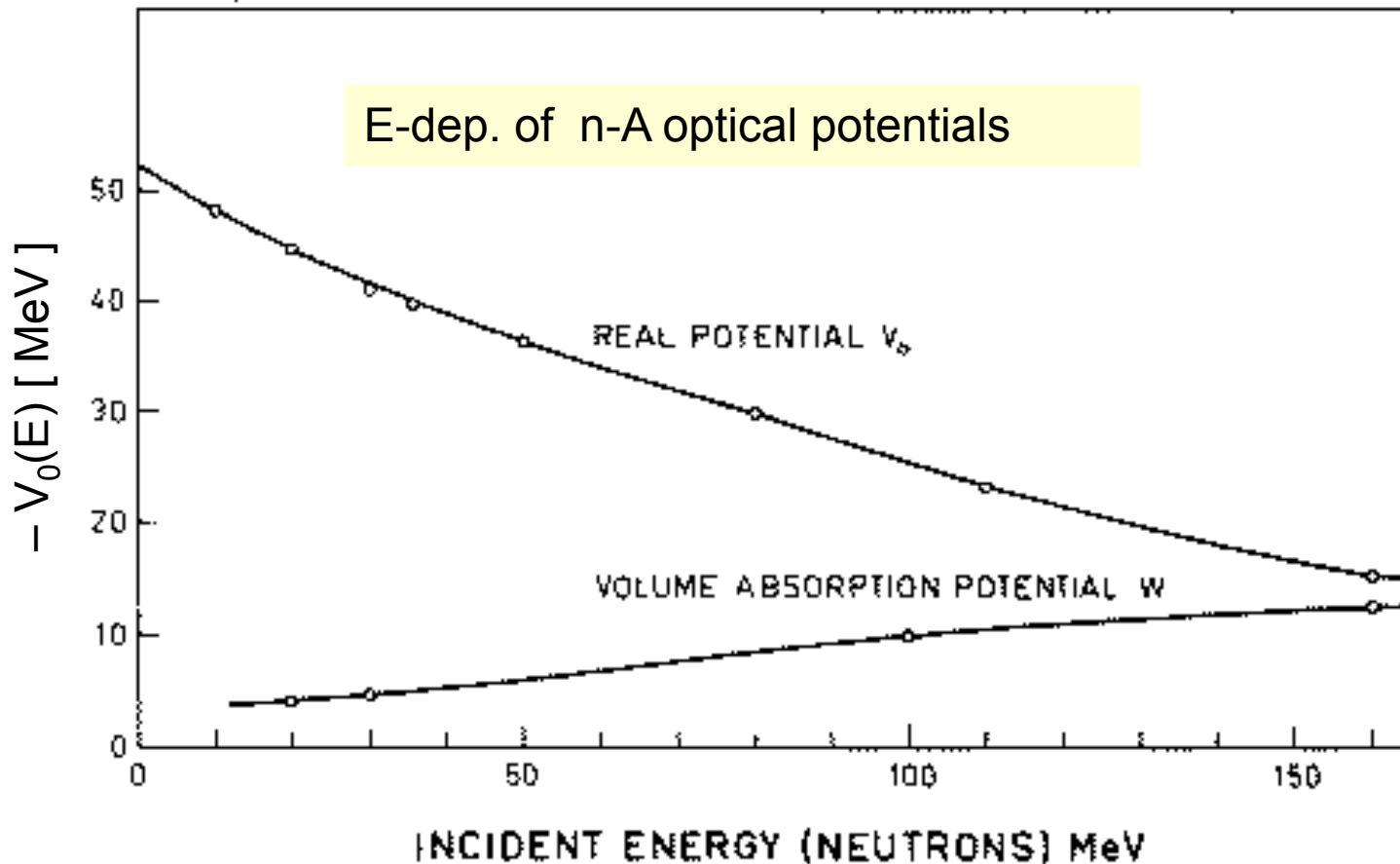
$$1j_{15/2}^{+1} \frac{15/2^-}{1.43}$$

$$2f_{7/2}^{+1} \frac{7/2^-}{0.90} \quad 1i_{11/2}^{+1} \frac{11/2^+}{0.78}$$

$$0^+ \quad 0.00 \quad 1h_{9/2}^{+1} \frac{9/2^-}{0.00} \quad 2g_{9/2}^{+1} \frac{9/2^+}{0.00}$$

$$^{208}_{82}\text{Pb}_{126} \quad ^{209}_{83}\text{Bi}_{126} \quad ^{209}_{82}\text{Pb}_{127}$$

光学ポテンシャル



低エネルギーの中性子に対して虚数部分は小さい

フェルミ気体(フェルミ液体)

- 飽和密度

- $\rho \approx 0.16 \text{ fm}^{-3} \Rightarrow k_F \approx 1.35 \text{ fm}^{-1}$

- フェルミ・エネルギー $T_F = \frac{\hbar^2 k_F^2}{2m} \approx 40 \text{ MeV}$

- $\Rightarrow k_F r \approx 1, \quad k_F a \gg 1$ 非希薄、強結合フェルミ系
有効レンジ、散乱長

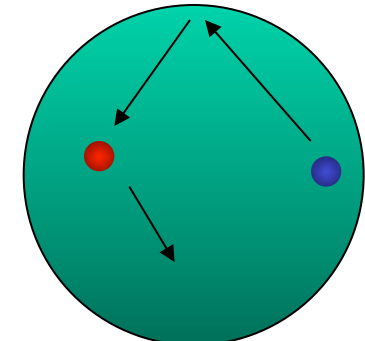
- 核子が核内で動き回る時間周期

$$\tau_F \approx \frac{R}{v_F} \sim 10^{-22} \text{ s}$$

- 核子・核子衝突時間

$$\tau_c \gg \tau_F$$

$$\lambda \gg R$$



準粒子(quasi-particle)による記述

中性子共鳴散乱

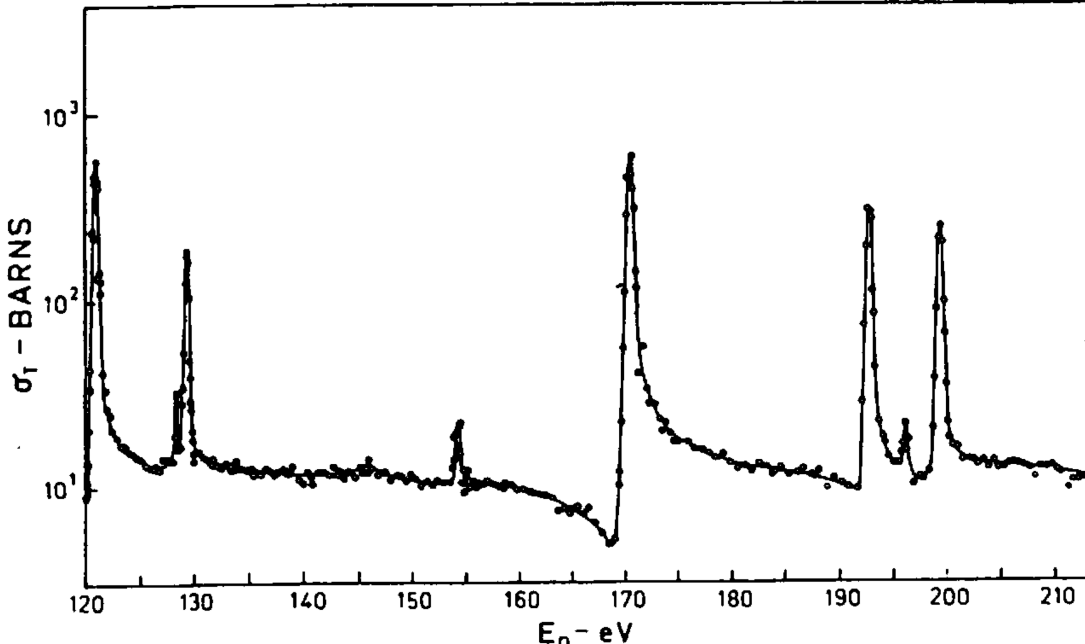
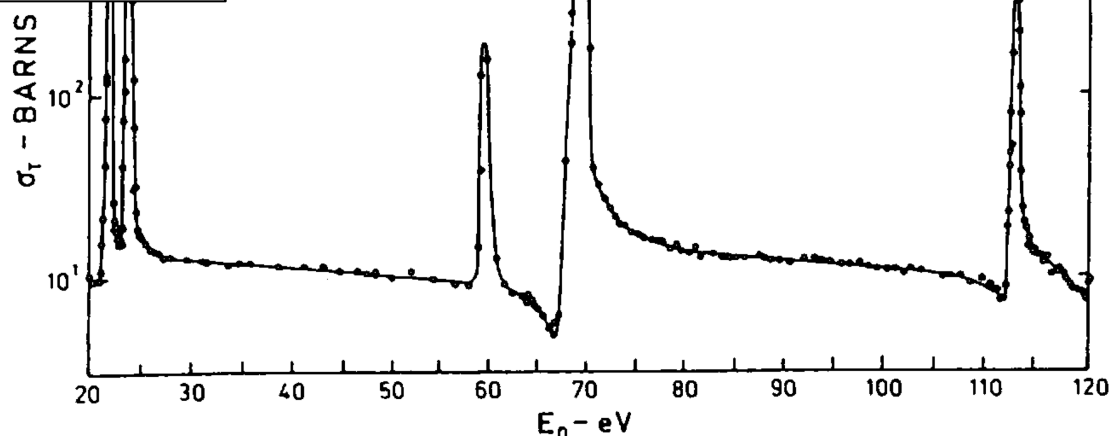
中性子にはクーロン反発力が働くため、容易に原子核に衝突

低エネルギーの熱中性子(eVオーダー)による散乱実験によって多数の共鳴状態が観測

$$\tau_{\text{comp}} \gg \tau_c$$

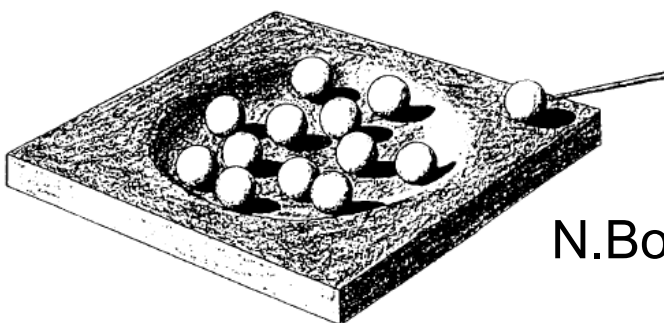
準粒子による記述は不可
エネルギー分解能に限界

$$\Delta E > \hbar / \tau_c$$

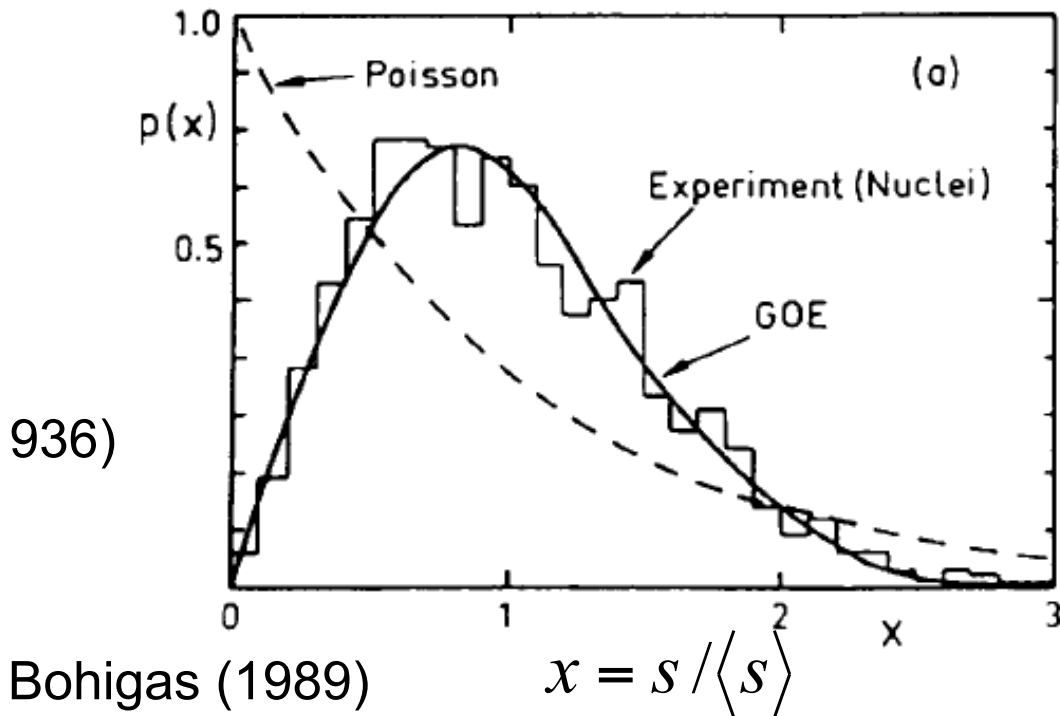


複合核模型 [Bohr 1936, Wigner, 1955]

- 熱中性子共鳴
 - 幅の小さい多数の共鳴状態 ($s \sim \text{eV}$, $\Gamma \sim \text{meV}$)
 - 準位間隔はウィグナー分布に従う(乱雑行列理論)
- 強結合・複雑系
 - 量子力オース的性質



N.Bohr (1936)



原子核集団運動

- 集団励起モードの時間スケール
 - “周期” $\tau_{\text{coll}} \sim \hbar/E_{\text{ex}}$
 - “寿命” $\tau_{\text{damp}} \sim \hbar/\Gamma$
 - Well-defined: $\tau_{\text{coll}} < \tau_{\text{damp}}$
 - 早い運動(短い時間)
 - 巨大共鳴
 - 強い減衰
 - 遅い運動(長い時間)
 - 低エネルギー振動モード
 - 核変形に伴う回転

早い集団励起の例：巨大四重極共鳴(GQR)

巨大共鳴：和則値(sum rule value)をほぼ100%尽くす状態

$$m_p = \sum_n E_n^p |\langle n | F | 0 \rangle|^2$$

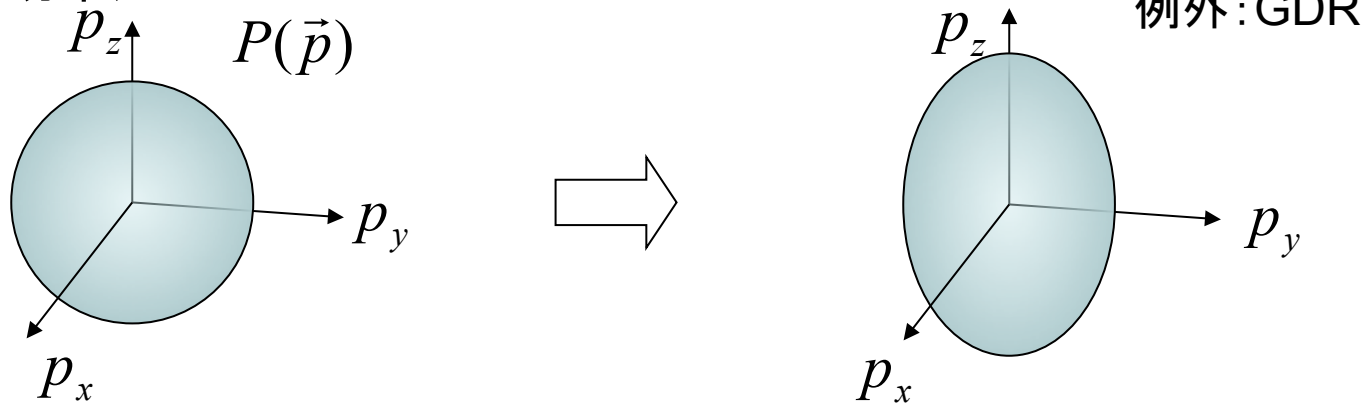
和則解析：復元力は3次の和則値に比例

cf) Ring-Schuck, Nuclear Many-body problems (1980)

$$H = \frac{1}{2B} \pi^2 + \frac{1}{2} C \alpha^2$$

$$C \sim m_3 \sim \langle T \rangle$$

形状変形が運動量空間のフェルミ球を変形させる→エネルギー増加
(量子フェルミ効果)



低エネルギーの集団運動では、フェルミ球を球形に保とうとする

遅い集団励起: 表面振動モード

- 低エネルギー振動励起モード

- 表面振動モード(球形核)

$$H = \sum_{\lambda\mu} \left(\frac{1}{2B_\lambda} \pi_{\lambda\mu}^2 + \frac{1}{2} C_\lambda \alpha_{\lambda\mu}^2 \right)$$

$$\Rightarrow \sum_{\mu} \left(\frac{1}{2B_2} \pi_{2\mu}^2 + \frac{1}{2} C_2 \alpha_{2\mu}^2 \right)$$

- 古典的非回転液滴模型

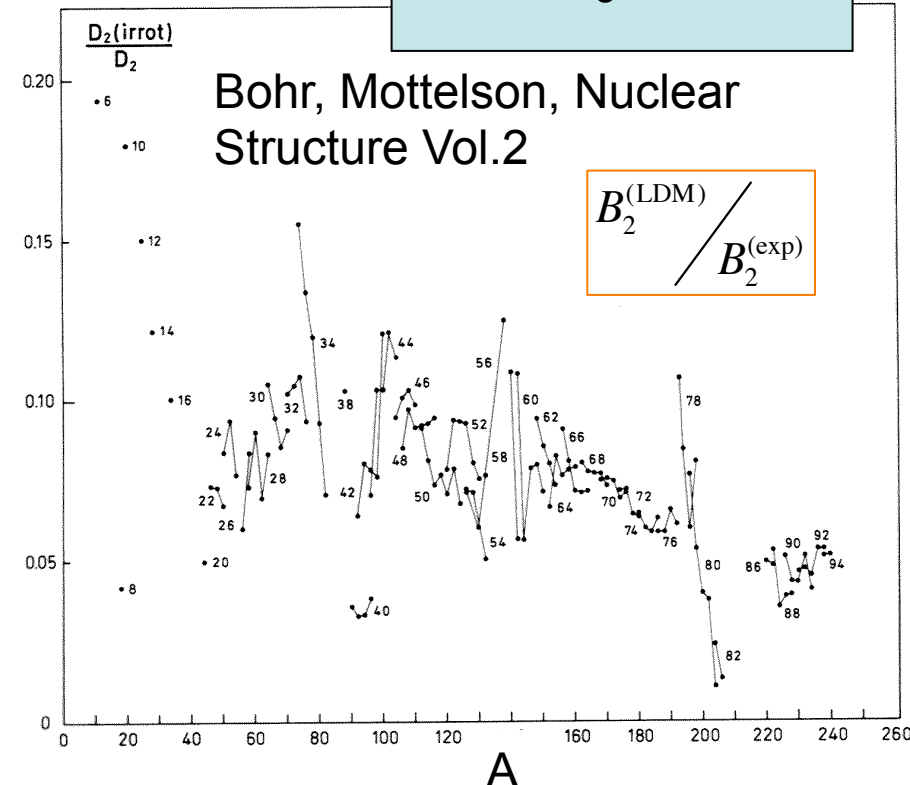
$$\lambda = 2 \quad C_2 = \pi^{-1} a_s A^{2/3} - \frac{3Z^2 e^2}{10\pi R_0}$$

$$B_2 = \frac{1}{2} M \rho_0 R_0^5$$

実験と非整合

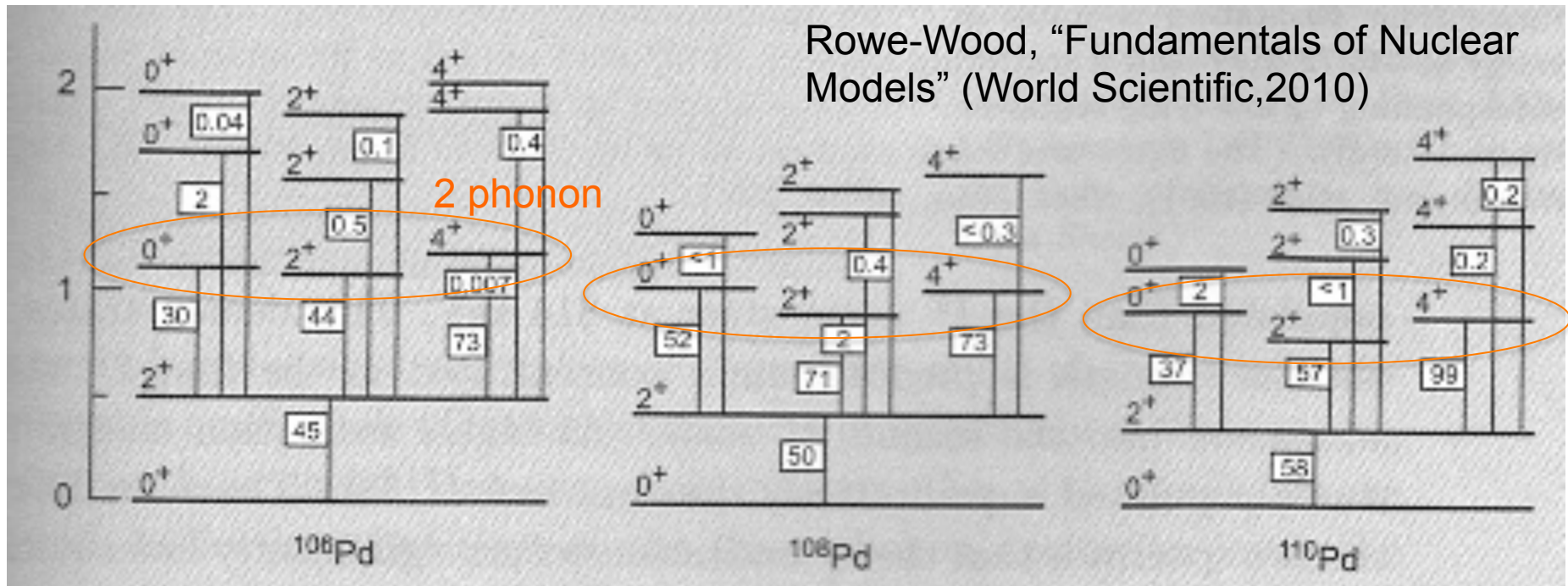
四重極振動

$\lambda = 2$
$0^+, 2^+, 4^+$
2^+
0^+

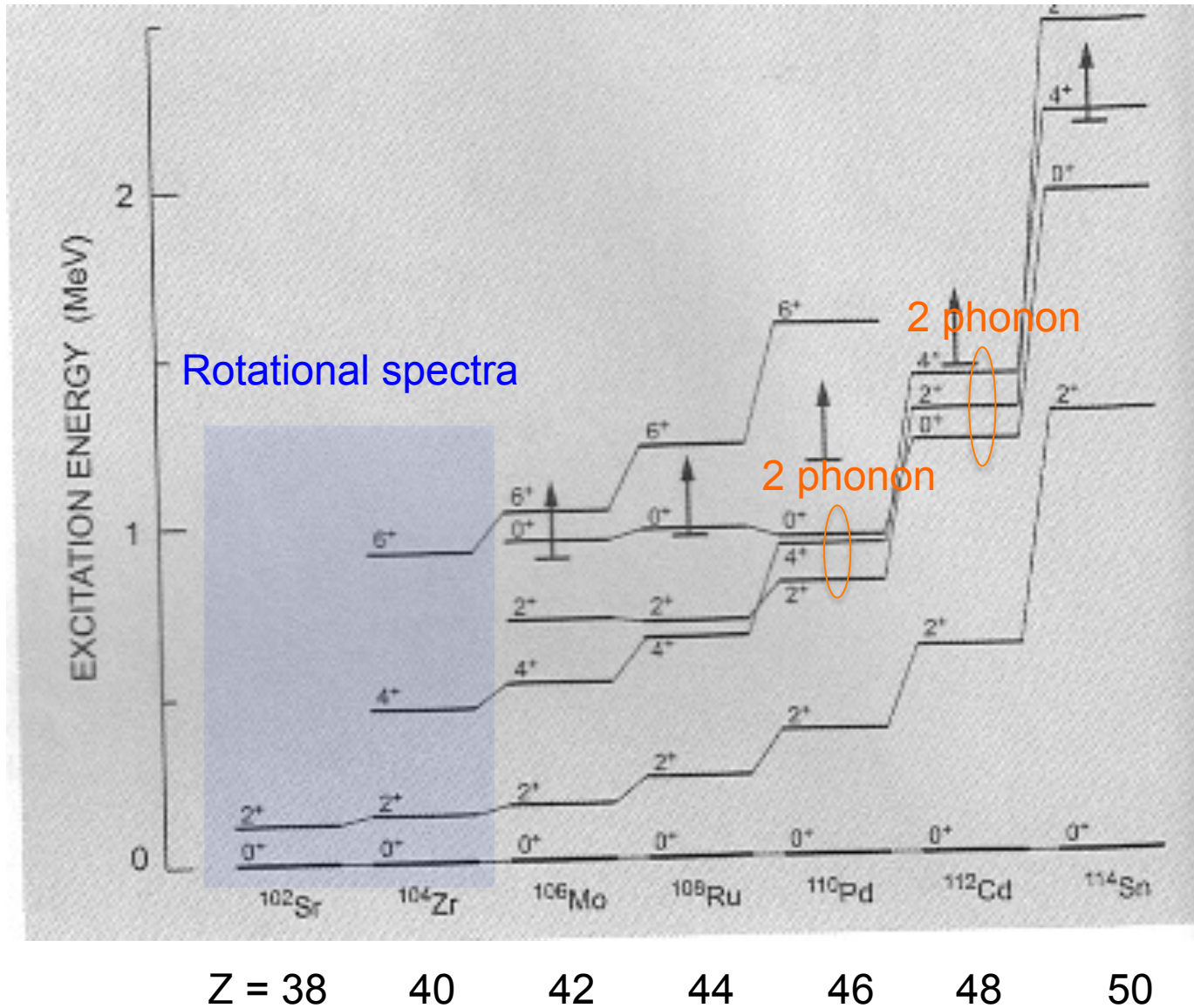


四重極振動励起

- 一重閉殻に比較的近い原子核(N, Z :偶数)
 - 例:Pd ($Z=46$ [$=50-4$])
 - 1振動子(1 phonon)状態 ($J^\pi = 2^+$)
 - 2振動子(2 phonon)状態 ($J^\pi = 0^+, 2^+, 4^+$)

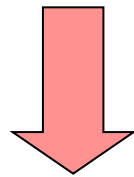


閉殻 → 開殻



フォノン凝縮による核変形

$|\Phi_0\rangle$ 球形の基底状態
 $B_{2^+}^+ |\Phi_0\rangle$ 1-phonon状態 (2^+)
 $[B_{2^+}^+ B_{2^+}^+]_M^L |\Phi_0\rangle$ 2-phonon状態 (L^+)

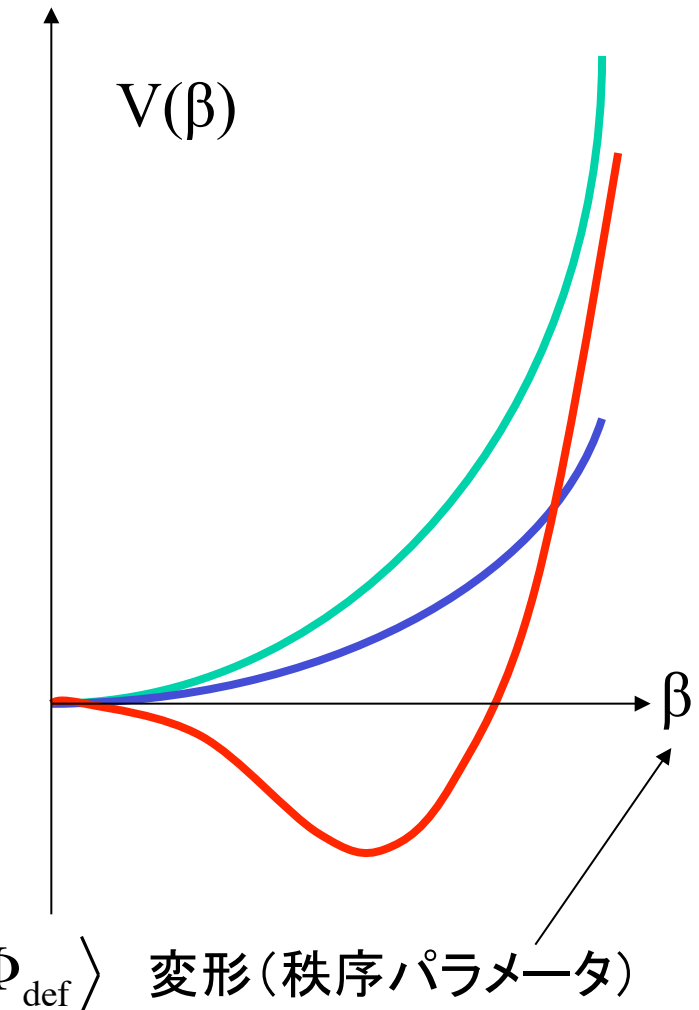


閉殻 → 開殻

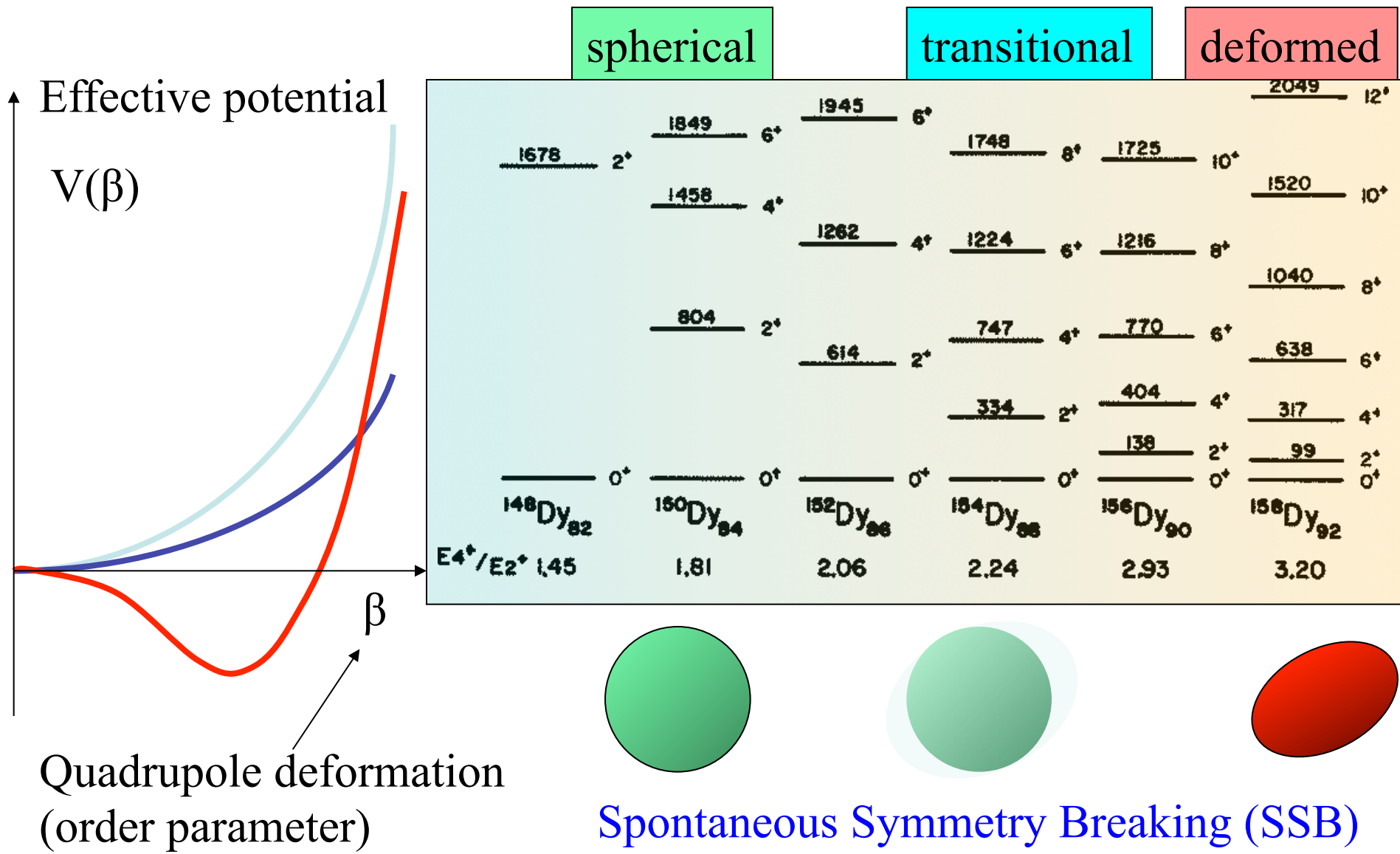
$$|\Phi_{\text{def}}\rangle \approx \exp(cB_{2^+}^+) |\Phi_0\rangle$$

$$\beta \sim \langle \Phi_{\text{def}} | B_{2^+}^+ | \Phi_{\text{def}} \rangle$$

$$\sim \langle \Phi_{\text{def}} | r^2 Y_{20}(\hat{r}) | \Phi_{\text{def}} \rangle$$



形状相転移

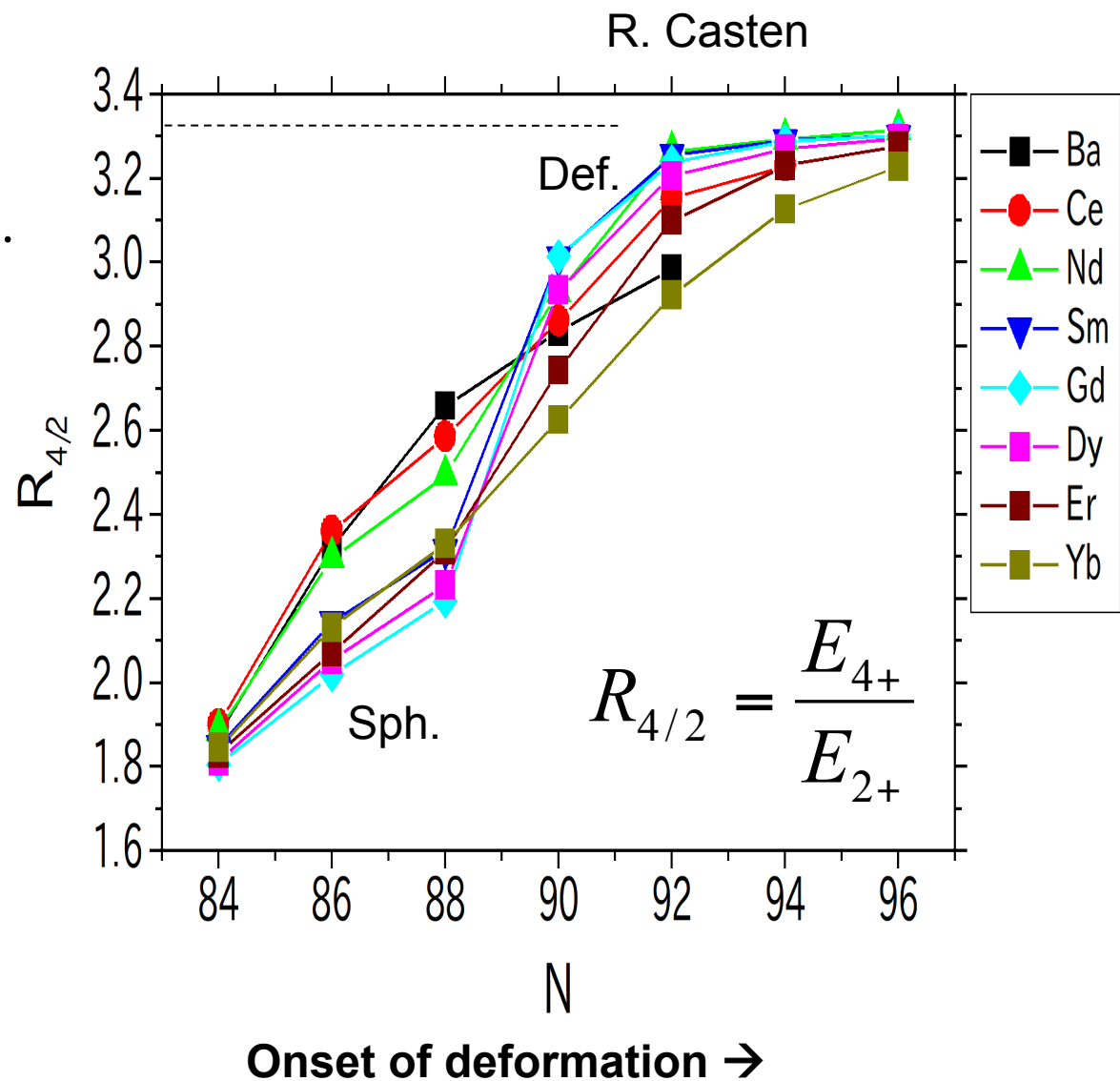


$R_{4/2}$ でみる変形の成長(実験データ)

$$E_I = \frac{I(I+1)}{2\mathfrak{J}}$$

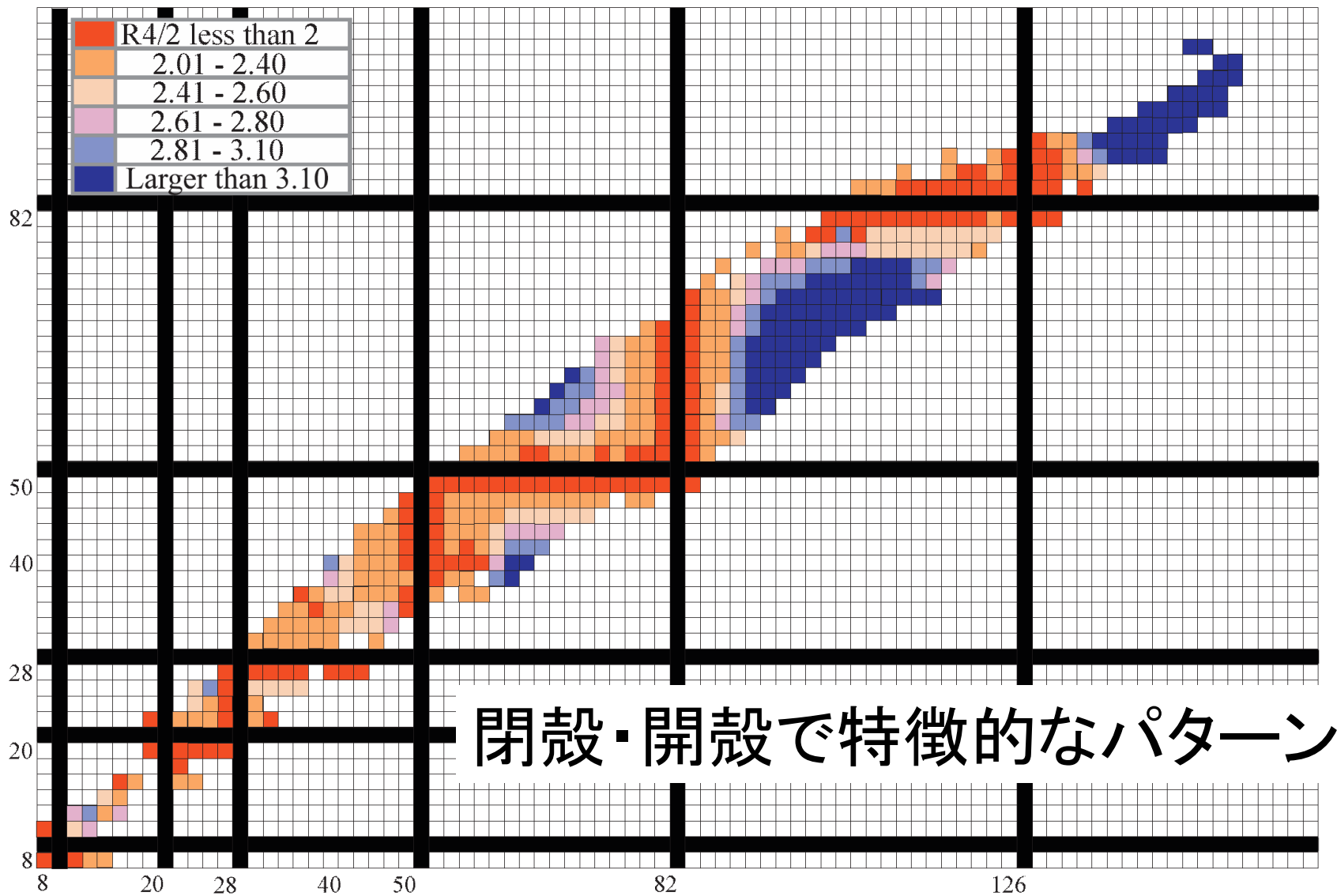
↓

$$R_{4/2} = \frac{E_4}{E_2} = \frac{20}{6} = 3.33\dots$$



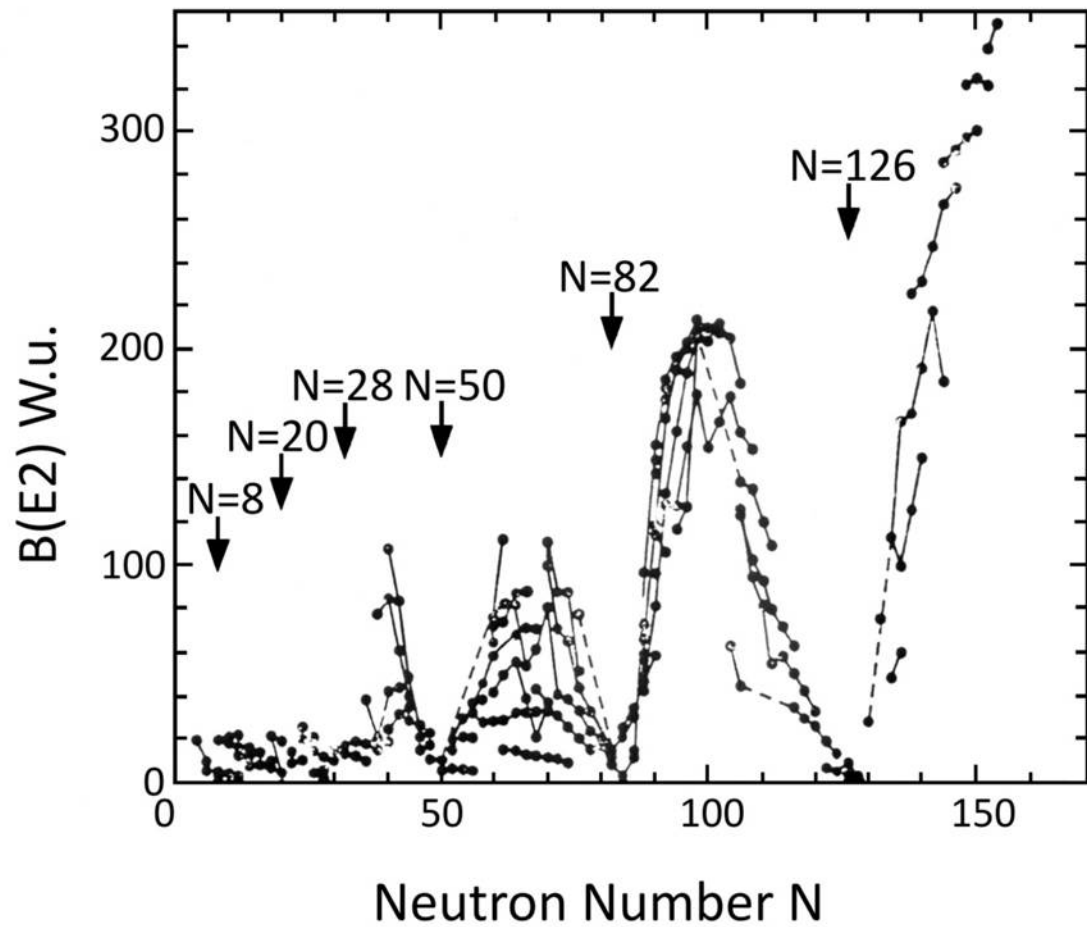
核図表(偶々核)における $R_{4/2}$

Courtesy: R. Casten



2^+ 0^+

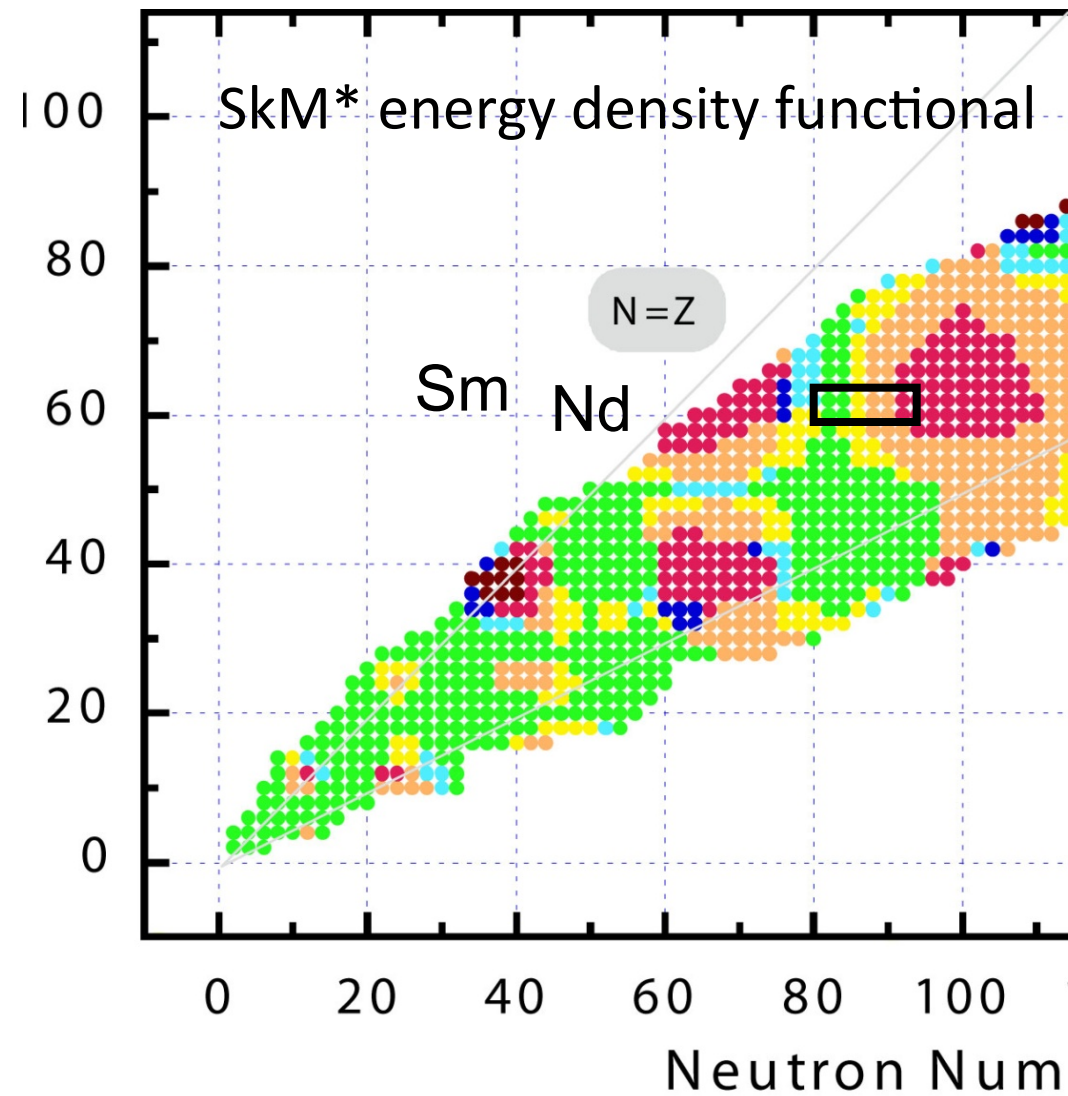
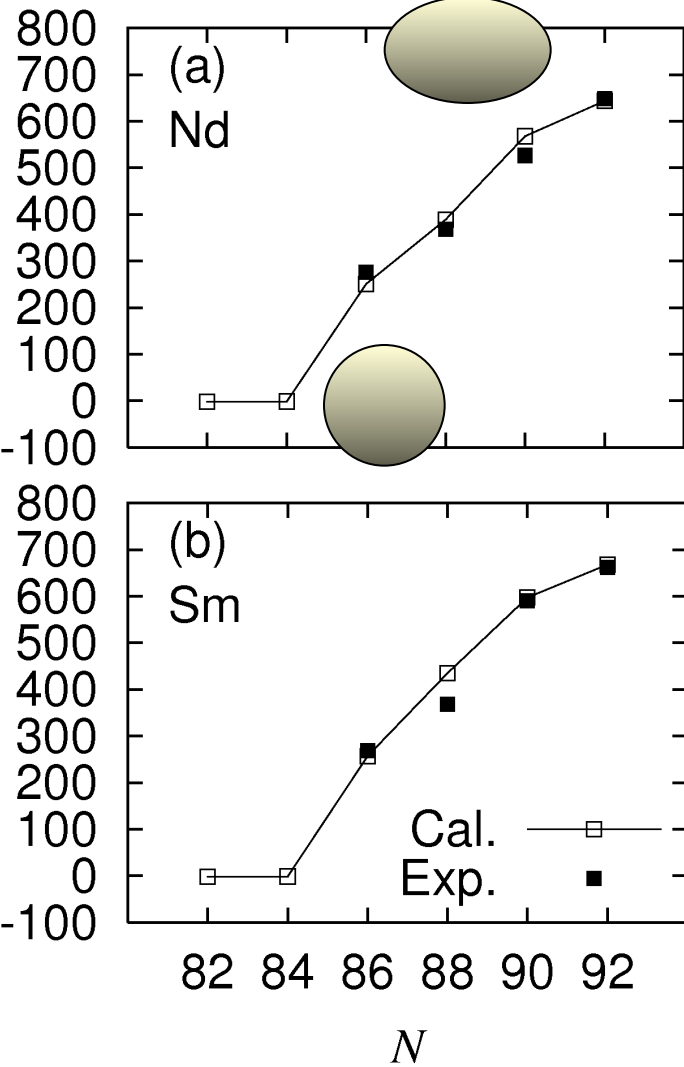
$$B(E2: 0^+_1 \rightarrow 2^+_1) \propto \langle 2^+_1 | | E2 | | 0^+_1 \rangle^2$$



密度汎関数計算による核変形の再現・予言

Intrinsic Q moment

$$\langle \hat{Q}_{20} \rangle$$



(時間依存)密度汎関数理論 [(TD)DFT]

- エネルギー密度汎関数

$$E[\rho_q(t), \tau_q(t), \vec{J}_q(t), \vec{j}_q(t), \vec{s}_q(t), \vec{T}_q(t); \kappa_q(t)]$$

↑ ↑ ↑ ↑ ↑ ↑
kinetic current spin spin-kinetic pair density
spin-current spin

- Time-dependent BdG Kohn-Sham eq.

$$i \frac{\partial}{\partial t} \begin{pmatrix} U_\mu(t) \\ V_\mu(t) \end{pmatrix} = \begin{pmatrix} h(t) - \lambda & \Delta(t) \\ -\Delta^*(t) & -(h(t) - \lambda)^* \end{pmatrix} \begin{pmatrix} U_\mu(t) \\ V_\mu(t) \end{pmatrix}$$

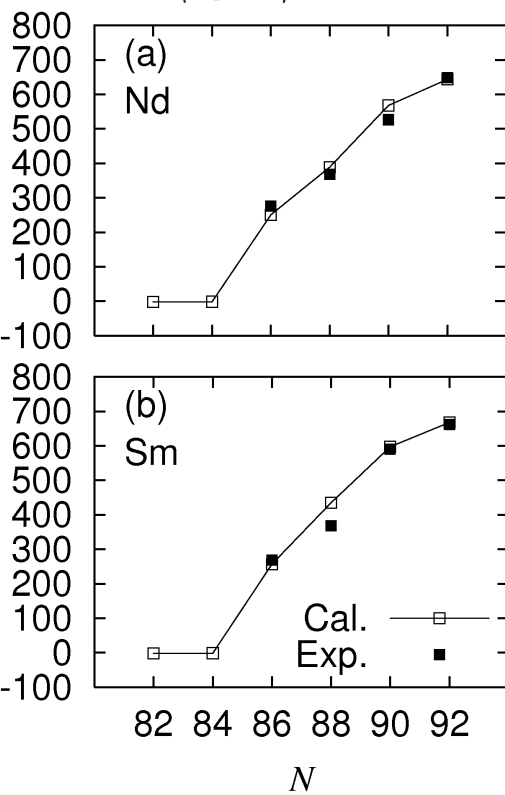
時間依存密度汎関数計算:光吸收断面積

SkM* functional

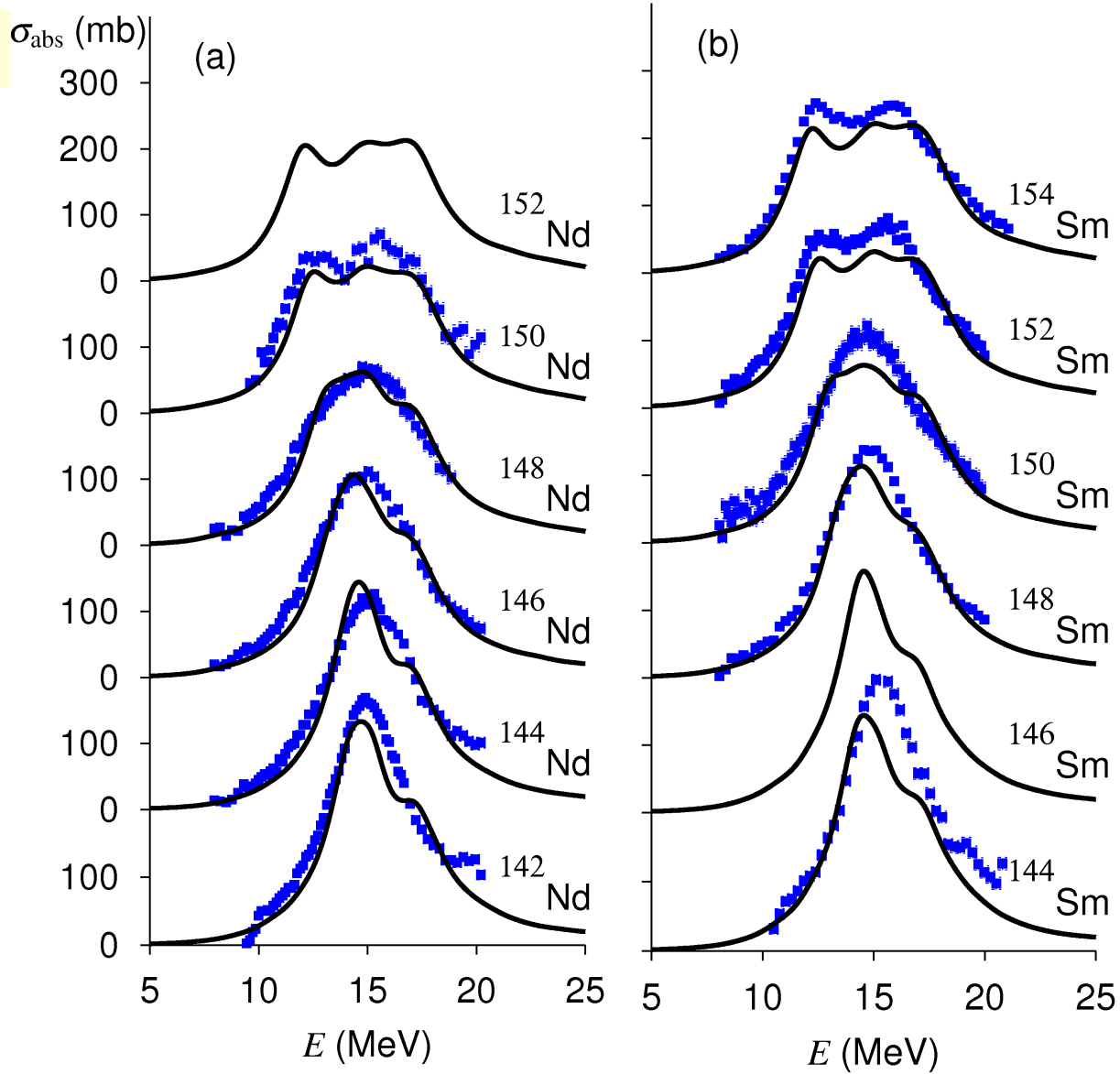
($S \sim 30$ MeV, $K \sim 217$ MeV)

Intrinsic Q moment

$$\langle \hat{Q}_{20} \rangle$$

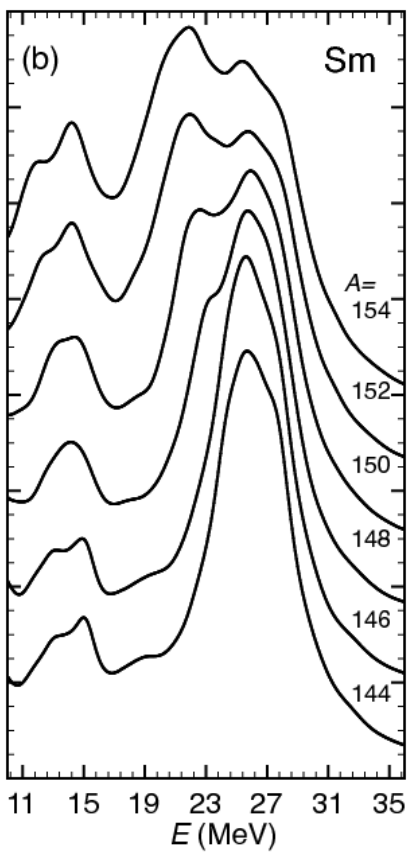
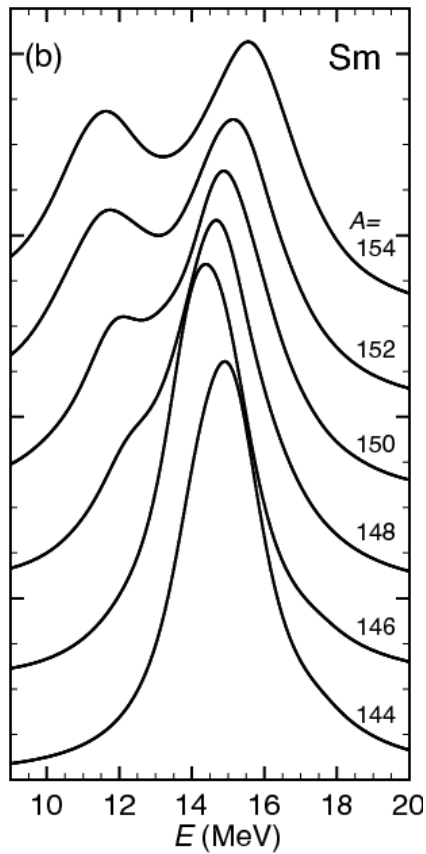


Yoshida, Nakatsukasa, PRC 83, 021304 (2011)



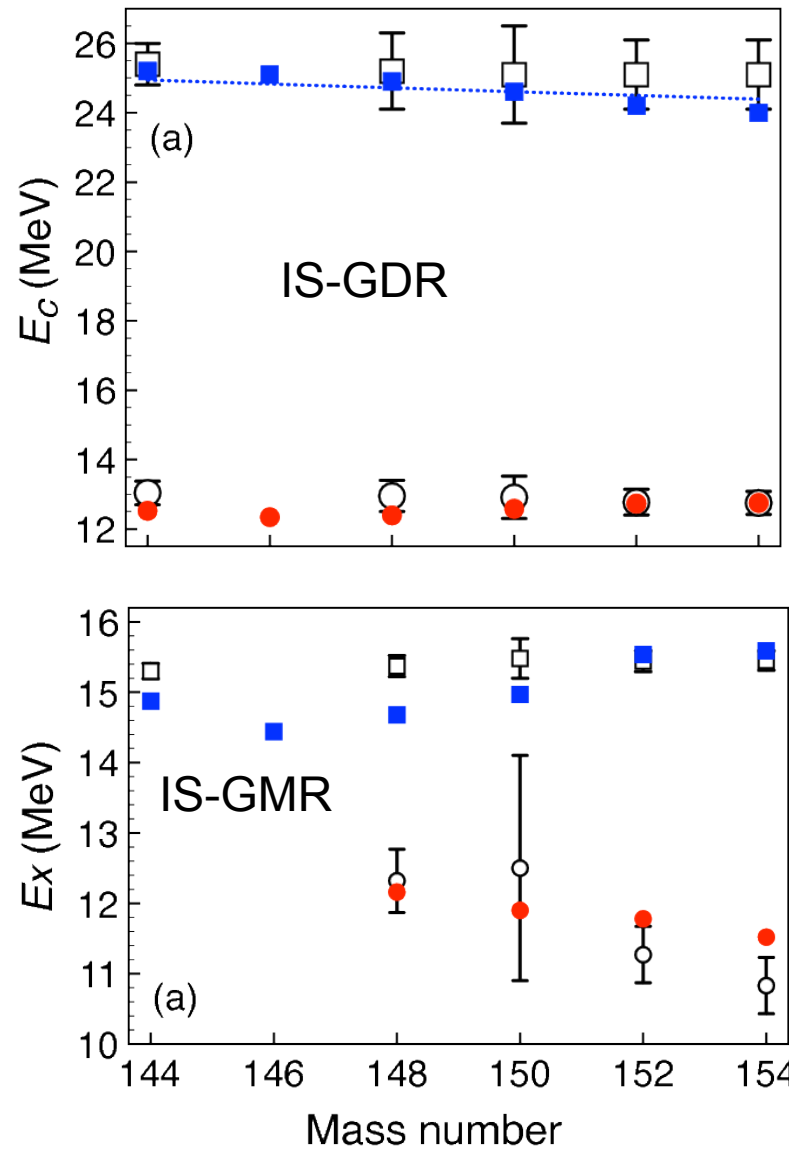
核変形と巨大共鳴(IS,IV; L=0~3)

IS-GMR



IS-GDR

Yoshida and TN, PRC88 (2013) 034309
スパコン「京」の成果 (hp120192)

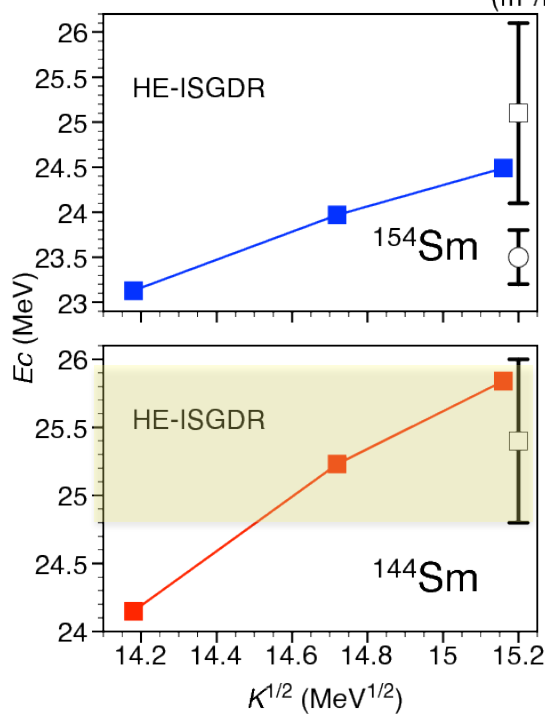
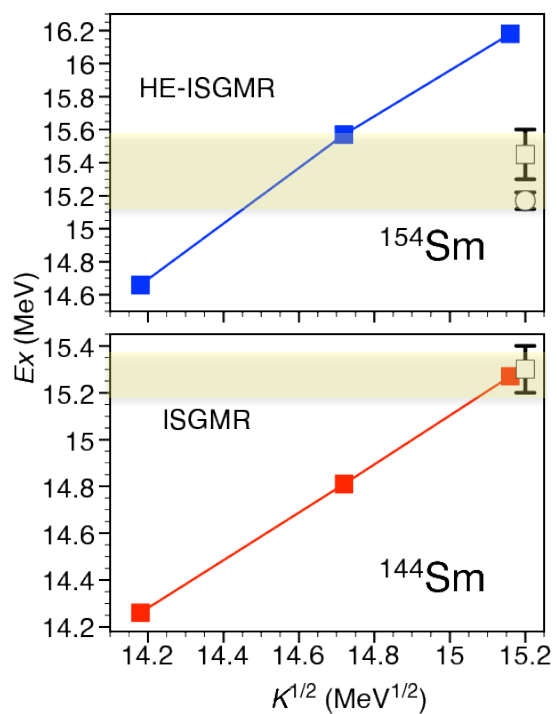
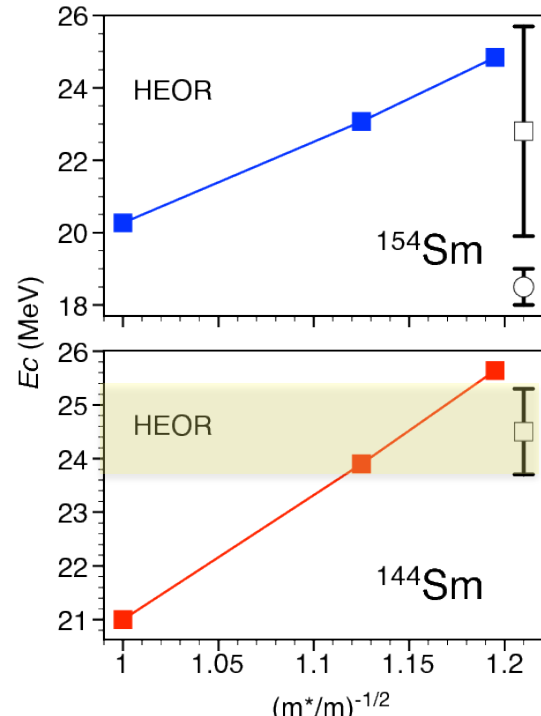
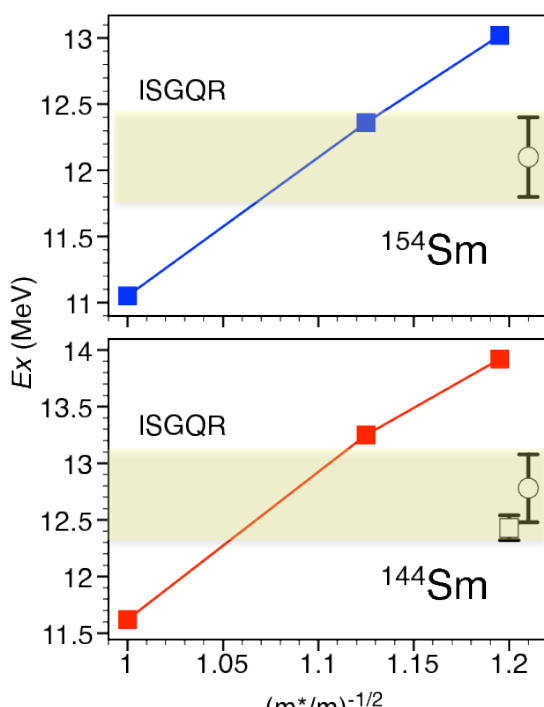


密度汎関数の比較

核子有効質量

$$\frac{m^*}{m} = 0.8 \sim 0.9$$

(ISGQRのデータより)



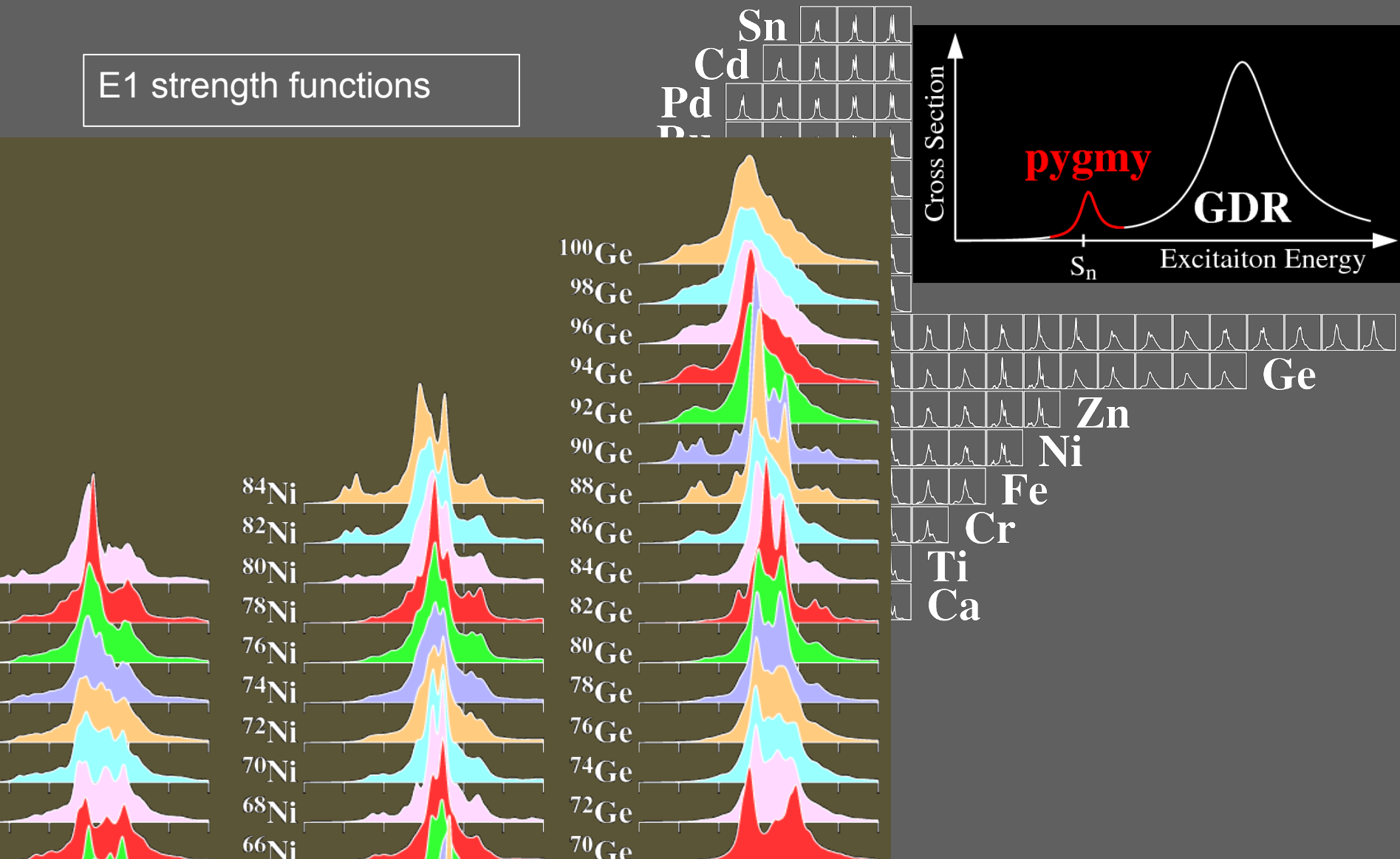
非圧縮率

$$K = 210 \sim 230 \text{ MeV}$$

Computational nuclear data tables

Inakura, T.N., Yabana, PRC 84, 021302 (R) (2011); arXiv: 1306.3089

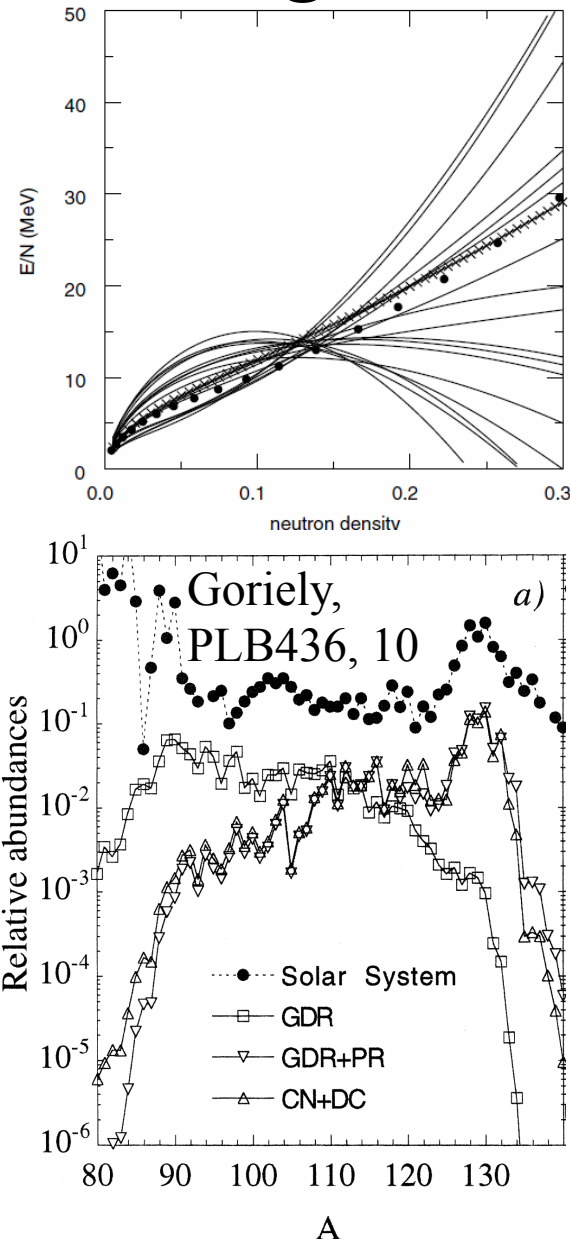
E1 strength functions



Issues in low-energy $E1$ strength

Inakura, et al., arXiv: 1306.3089

- Does the observation constrain the neutron skin thickness and the neutron-matter EOS?
 - Yes, but we need to go to very neutron rich!
 - ^{84}Ni is much better than ^{68}Ni
- Does it influence the r-process?
 - Significantly influence the direct neutron capture process near the neutron drip line
 - We need calculation with a proper treatment of the continuum.



原子核の変形と対称性の自発的破れ

- 原子は“丸い”
 - 量子系
 - 零点運動エネルギーをなるべく下げる
- 分子は原子配置による変形
 - 古典系
- 原子核は分子とは違うメカニズムで変形
 - 量子系

分子の変形

分子	水素	水	アンモニア	メタン	二酸化炭素	窒素	エチレン
分子式	H ₂	H ₂ O	NH ₃	CH ₄	CO ₂	N ₂	C ₂ H ₄
電子式	H:H	H:[O]:H	H:[N]:H H	H:C:H H	:O::C::O:	:N::N:	H:C::C:H H H
構造式	H-H	H-O-H	H-N-H H	H-C-H H	O-C-O	N=N	H-C-C-H H H
分子モデル							
立体構造							
	直線形	折れ線形	三角すい形	正四面体形	直線形	直線形	平面形

- 分子配置による変形(古典的)
 - 慣性能率は剛体値

核力と原子間力

Bohr, Mottelson, Nucl. Str. Vol.1

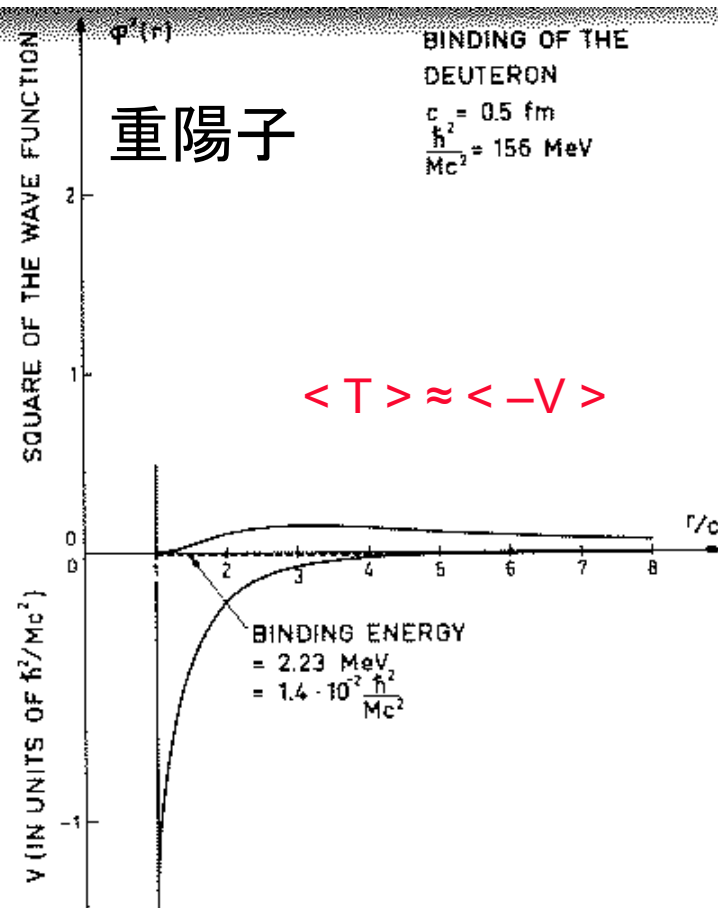
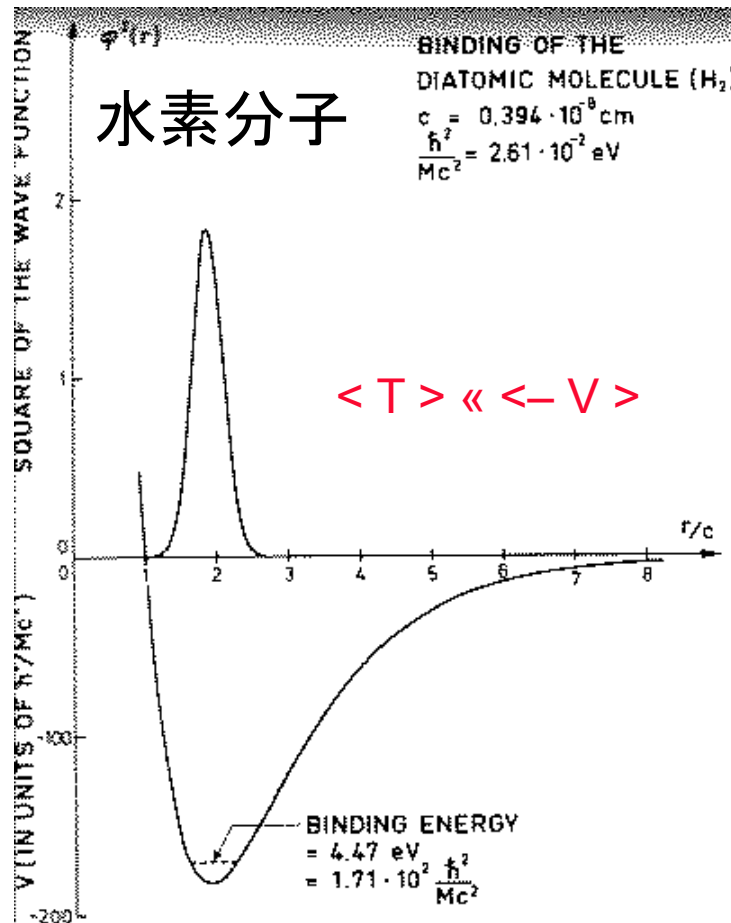


Figure 2.36. The molecular interaction corresponds to a "Morse potential" (Eq.(2.11) and Fig. 2.12) with the constants adjusted

低温で結晶化

古典的

低温で液体

量子的

量子流体としての原子核

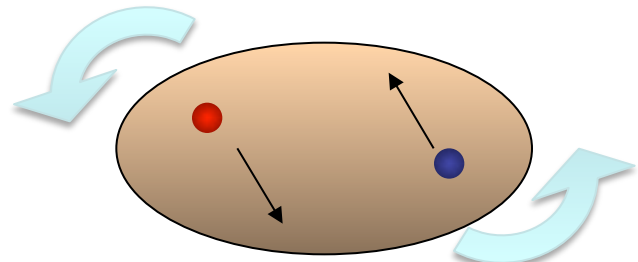
- 量子性の判定パラメータ
 - V_0 : 相互作用の強さ
 - c : 相互作用レンジ
- 典型的な系における値
 - 重い原子は以下よりもはるかに小さい値

$$\Lambda = \frac{\hbar^2}{2Mc^2} \cdot \frac{1}{V_0}$$

	Λ	絶対零度の相
水素(H)	0.06	固体
ヘリウム(${}^3\text{He}$, ${}^4\text{He}$)	0.1~0.2	液体
核子(n,p)	0.5	液体

有限量子系・原子核における変形

- 変形は有限の時間 τ_{SSB} において実現
 - フェルミ運動の周期時間 τ_F より十分長い
 - 通常、核子衝突時間 τ_c よりも短い
 - 核子は変形した核内を自由に高速で運動
$$v_F \sim 0.3c$$
- τ_{SSB} より長い時間では、量子的零点運動(zero-point motion)によって球形の密度分布に
 - 有限の相関時間 τ_{SSB}
 - 回転運動(集団運動)の出現
 - 実験で観測(回転スペクトル)

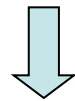


Rotating objects in the universe

Nucleus is one of the fastest rotating many-body system.

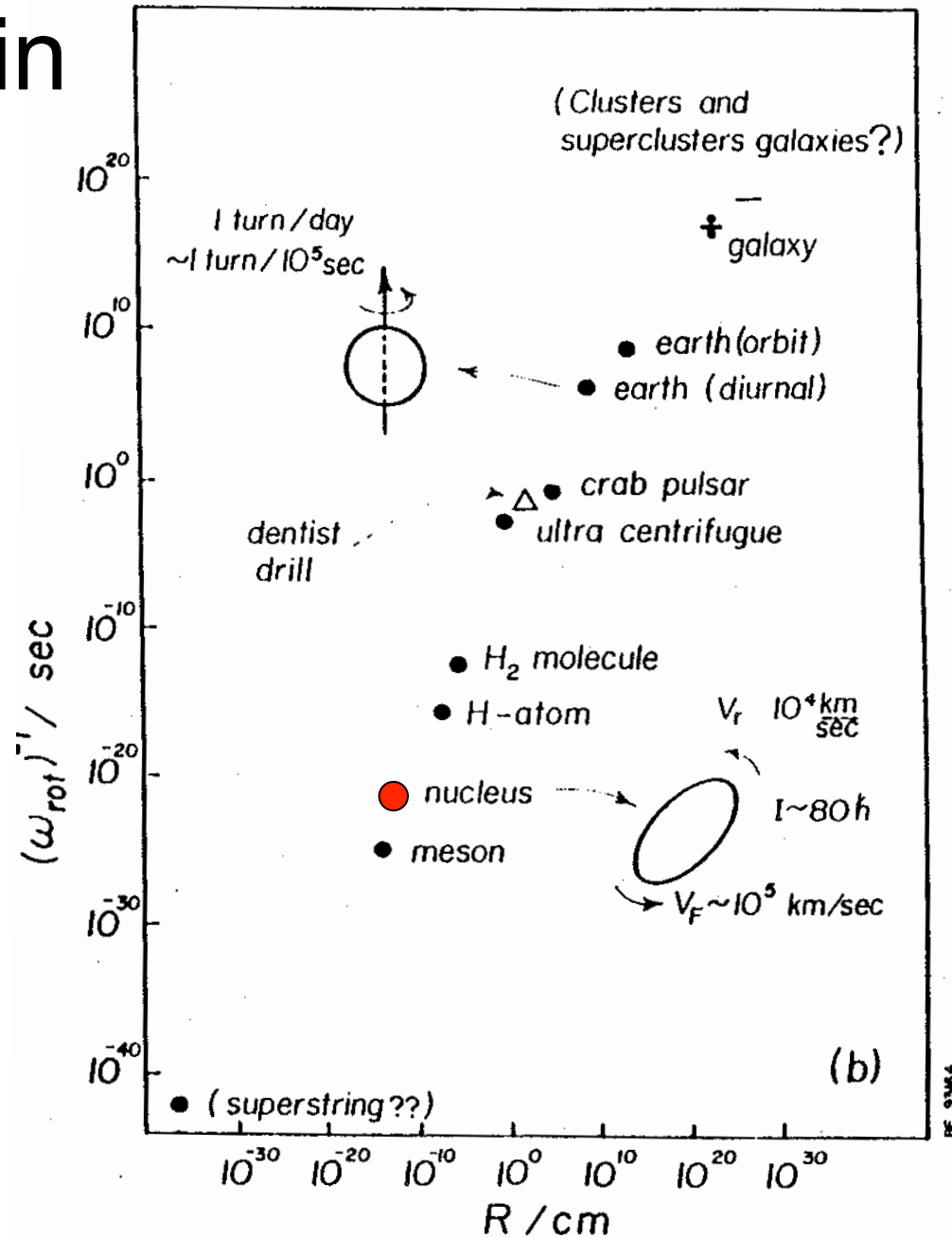
$$\frac{R_0 \omega_{\text{rot}}}{v_F} \ll 1 \quad \text{Low spin}$$

“Perturbative” Coriolis effects



$$\frac{R_0 \omega_{\text{rot}}}{v_F} \sim 1 \quad \text{High spin}$$

Non-perturbative Coriolis effects
Structure change, band crossings



Cranking model

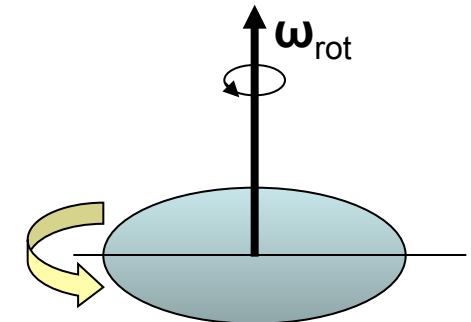
Picture in the rotating frame

Time-dependent Schrödinger equation

$$i \frac{\partial}{\partial t} |\Psi(t)\rangle = H |\Psi(t)\rangle$$

In the uniformly rotating frame with the rotational frequency ω

$$|\Psi(t)\rangle = e^{-i\omega t \cdot \mathbf{J}} |\Phi(t)\rangle \quad i \frac{\partial}{\partial t} |\Phi(t)\rangle = (H - \boldsymbol{\omega} \cdot \mathbf{J}) |\Phi(t)\rangle$$



Choose the rotational axis as x-axis: “1-dim. cranking”

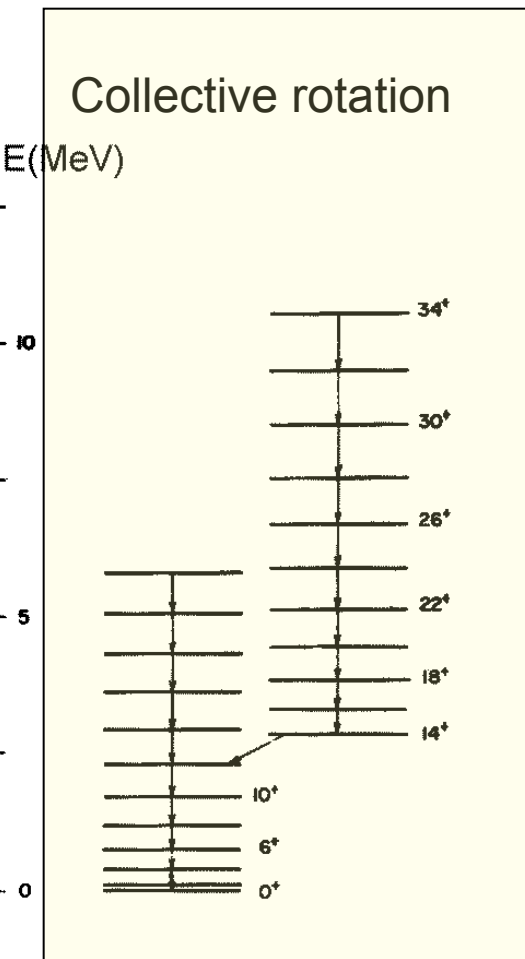
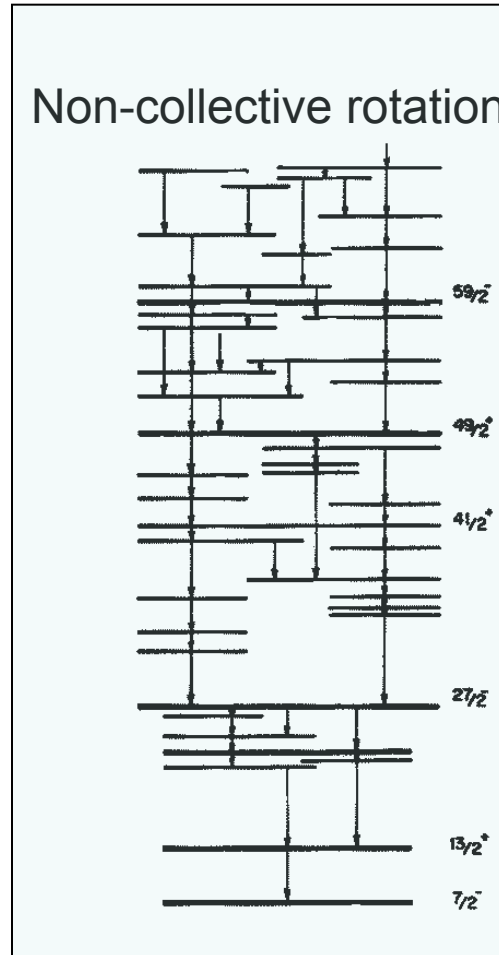
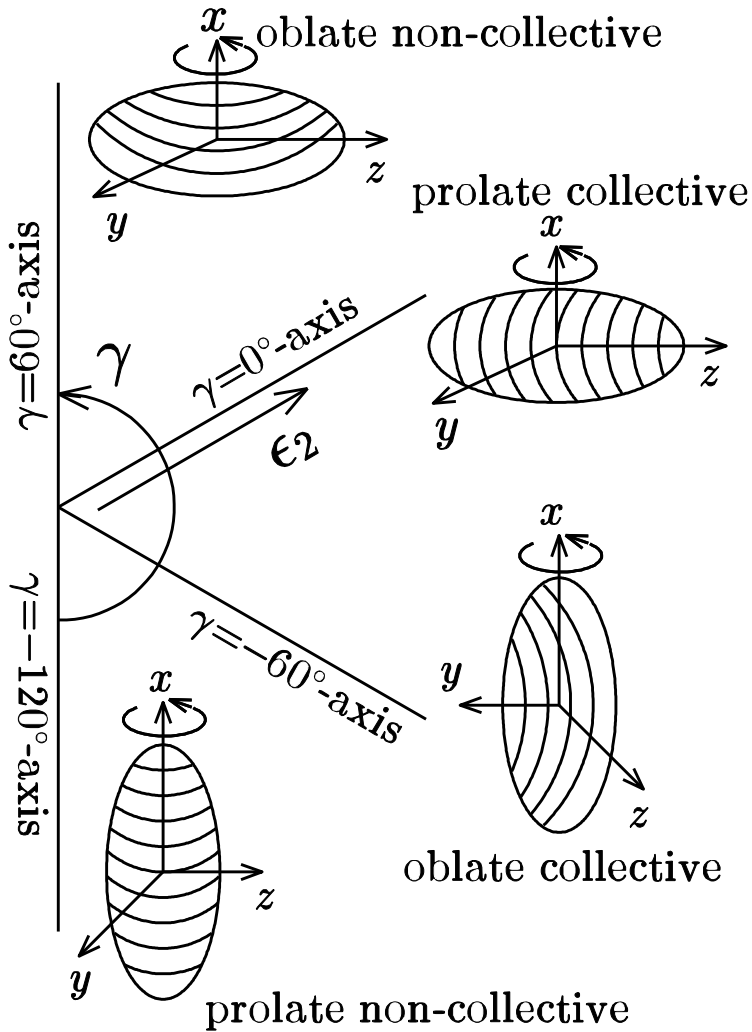
$$H' \equiv H - \boldsymbol{\omega} \cdot \mathbf{J} \Rightarrow H' = H - \omega_{\text{rot}} J_x$$

Cranking violates the time-reversal symmetry. However, in case of quadrupole deformation, it conserves the parity and signature symmetry:

$$\hat{R}_x = e^{-i\pi J_x} \quad r = e^{-i\pi\alpha}, \quad r = \begin{cases} \pm i, & \alpha = \mp \frac{1}{2} \\ \pm 1, & \alpha = \begin{cases} 0 \\ 1 \end{cases} \end{cases}$$

Experimentally, often defined as
 $\alpha = I \pmod{2}$

Collective and non-collective rotations



Cranking model is applicable to both cases.

Quasi-particle routhians

Quasi-particle eigen-energies of the “cranked” HFB equation

$$\begin{pmatrix} h - \lambda N - \omega_{\text{rot}} j_x & \Delta \\ -\Delta & -(h - \lambda N - \omega_{\text{rot}} j_x) \end{pmatrix} \begin{pmatrix} U \\ V \end{pmatrix} = e' \begin{pmatrix} U \\ V \end{pmatrix}$$

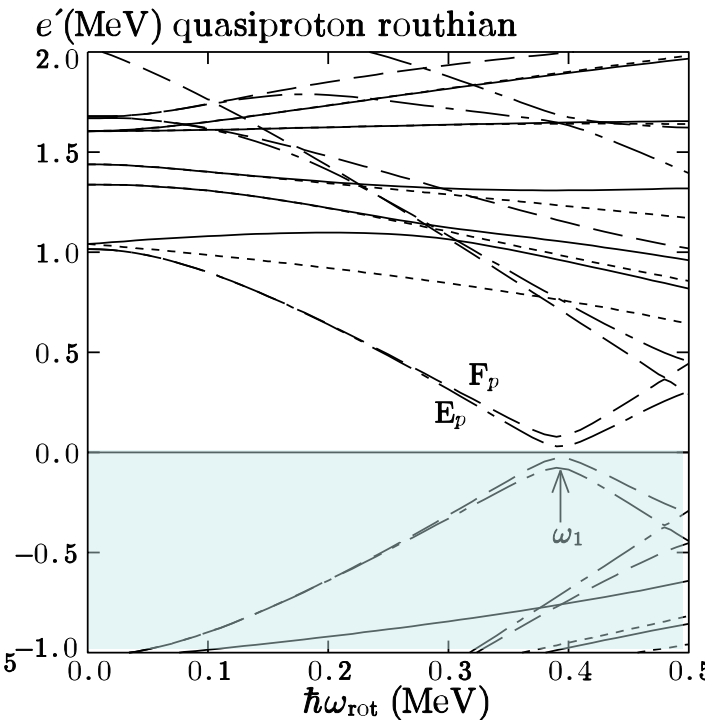
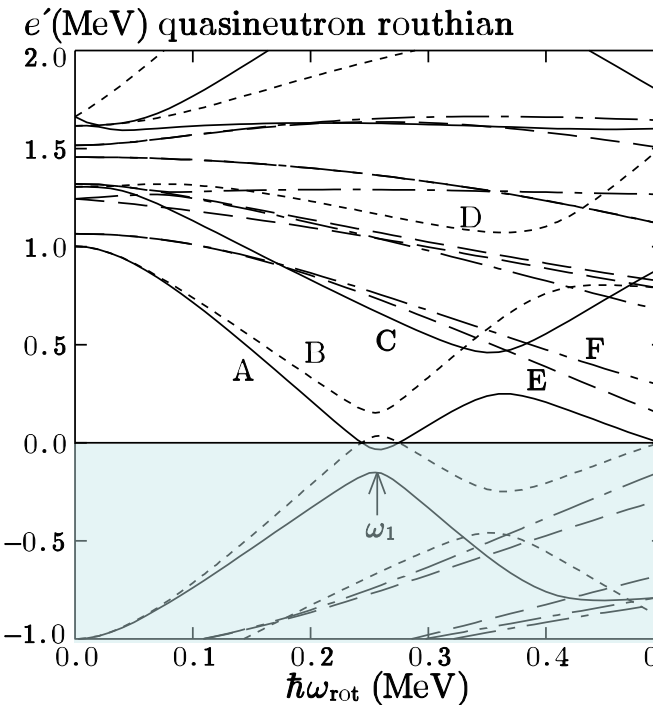
Even nuclei: qp vacuum \rightarrow ground band $E' = 0$

2qp excitation $e_A'(\omega) + e_B'(\omega), \dots$

Odd nuclei: 1qp exc. $e_A'(\omega), e_B'(\omega), \dots$

QP routhians
around ^{164}Er

Negative-energy states
are *fully occupied* in
the vacuum.

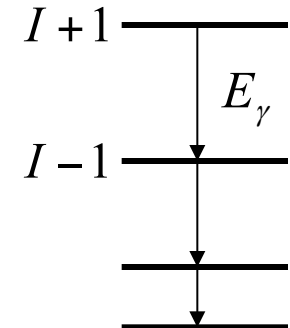


Experimental routhians

Angular momentum → Rotational frequency

$$\omega_{\text{rot}}(I) \equiv \frac{dE}{dI} \approx \frac{E(I+1) - E(I-1)}{I_x(I+1) - I_x(I-1)} \approx \frac{E_\gamma(I+1 \rightarrow I-1)}{2}$$

$$I_x(I) = \sqrt{(I+1/2)^2 - K^2}$$



Routhian and relative routhian

$$E'(\omega_{\text{rot}}) = E(I) - \omega_{\text{rot}} I_x(I) \approx \frac{1}{2} [E(I+1) + E(I-1)] - \frac{\omega_{\text{rot}}}{2} [I_x(I+1) + I_x(I-1)]$$

$$e'(\omega_{\text{rot}}) \equiv E'(\omega_{\text{rot}}) - E'_{\text{ref}}(\omega_{\text{rot}})$$

Ground-state band as the reference band

$$I_x(\omega_{\text{rot}}) = J_0 \omega_{\text{rot}} + J_1 \omega_{\text{rot}}^3 \quad \text{The Harris formula parameters are determined by fitting}$$

$$E'_{\text{ref}}(\omega_{\text{rot}}) = - \int I_x(\omega) d\omega = E'_0 - \frac{1}{2} J_0 \omega_{\text{rot}}^2 - \frac{1}{4} J_1 \omega_{\text{rot}}^4$$

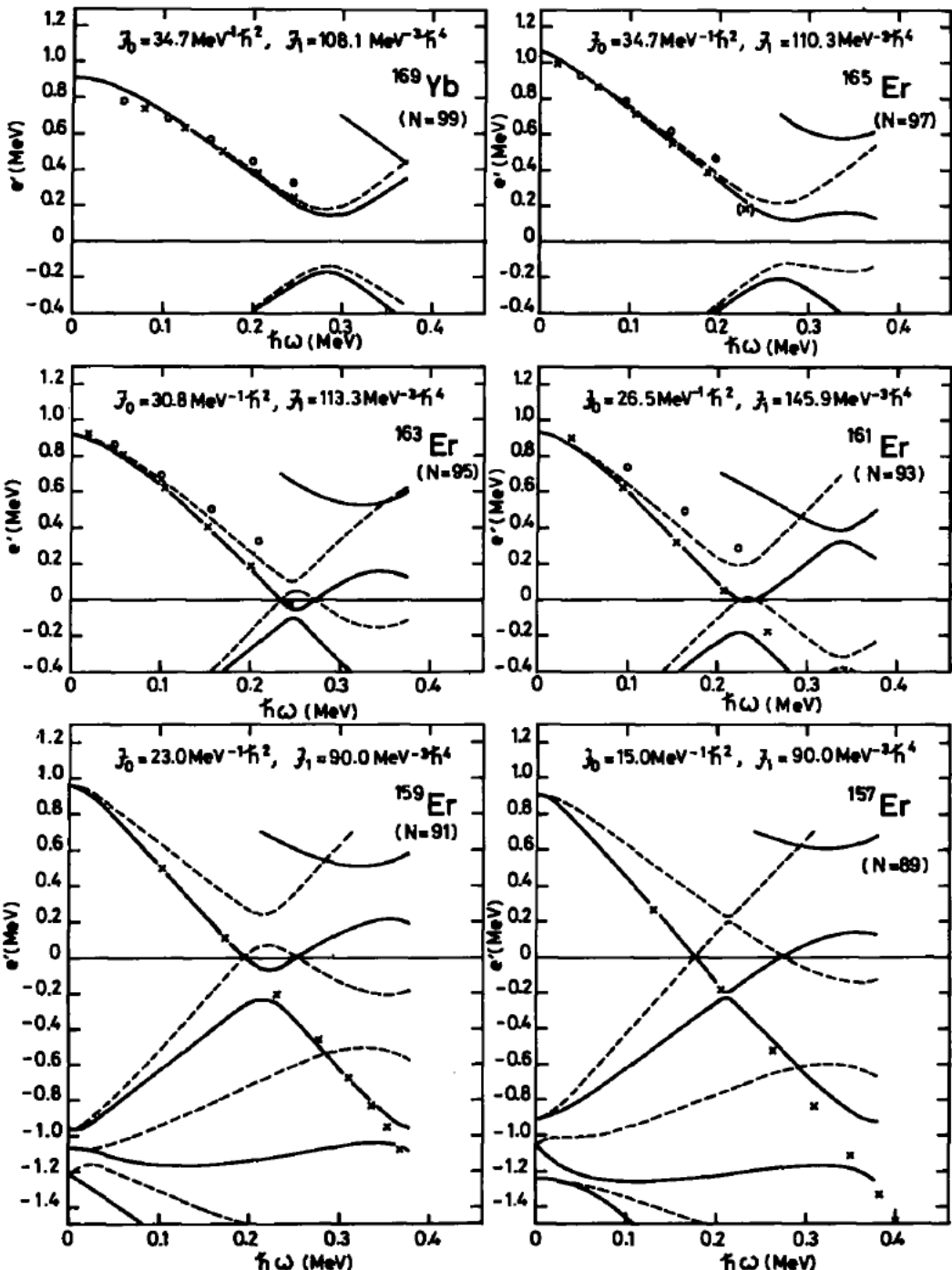
The “const.” is chosen so as to make the ground state ($I=0$) at zero energy.

$$E'_0 = \frac{1}{8J_0}$$

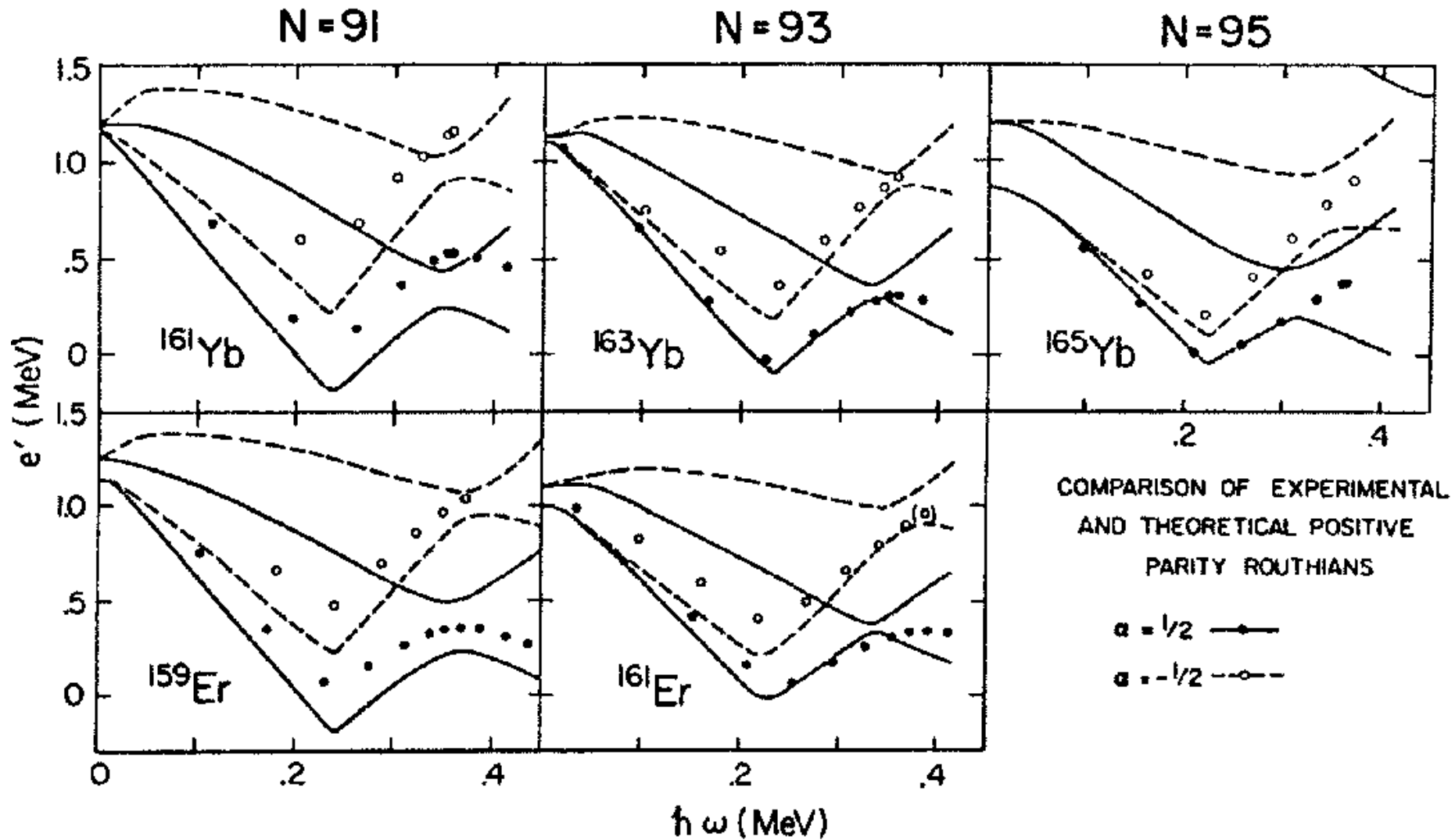
Routhian analysis

Bengtsson & Frauendorf, NPA327
(1979) 139.

Experimental quasi-particle
routhians in odd rare-earth nuclei

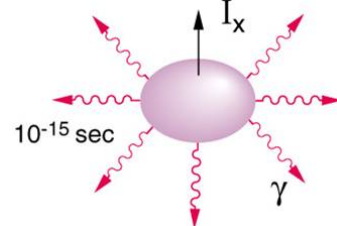


We may take, as the reference routhians, the experimental yrast routhians of neighboring even-even nuclei (or their average).



Back-bending phenomena

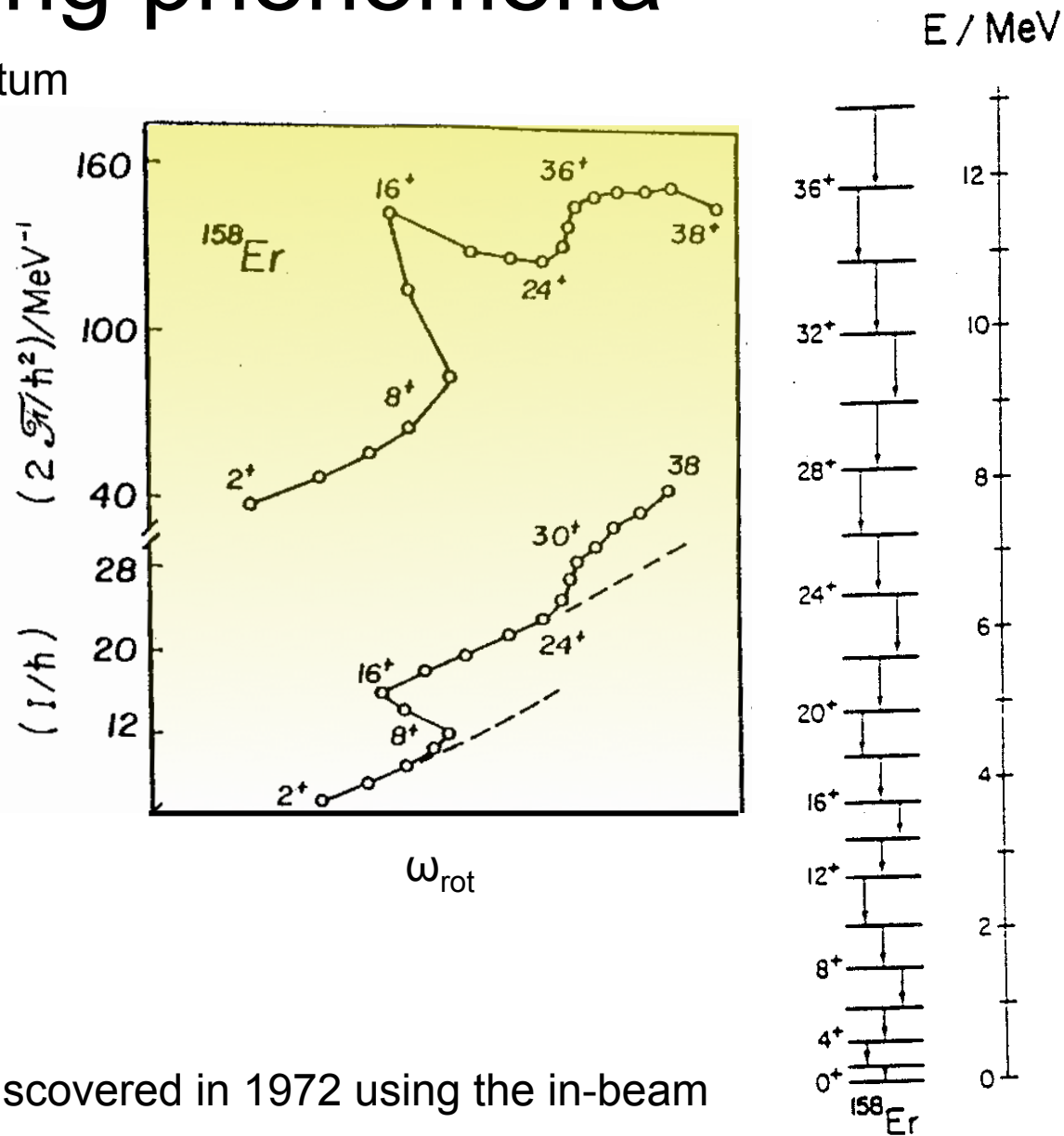
Nucleus loses its angular momentum by emitting gamma rays.



The ^{158}Er nucleus is spinning down, losing $\Delta I=2$ each step.

But, then, at $I=16$, it spins up, even though losing the angular momentum.

“Nuclear glitch”

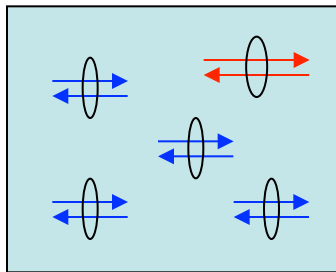


This phenomenon was first discovered in 1972 using the in-beam gamma-ray spectroscopy.

Structure change of the yrast states

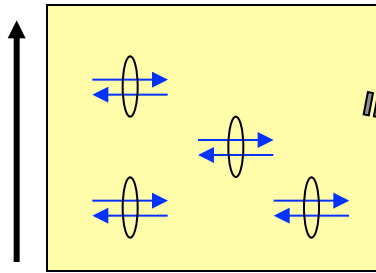
At low spin, the Cooper pair is condensed in the ground state.

$$|\Phi_{\text{HFB}}\rangle \approx \left(\sum_k \alpha_k c_k^+ c_{\bar{k}}^+ \right)^{N/2} |0\rangle$$

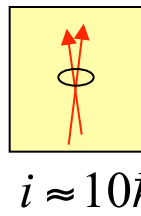


↑ Coriolis force

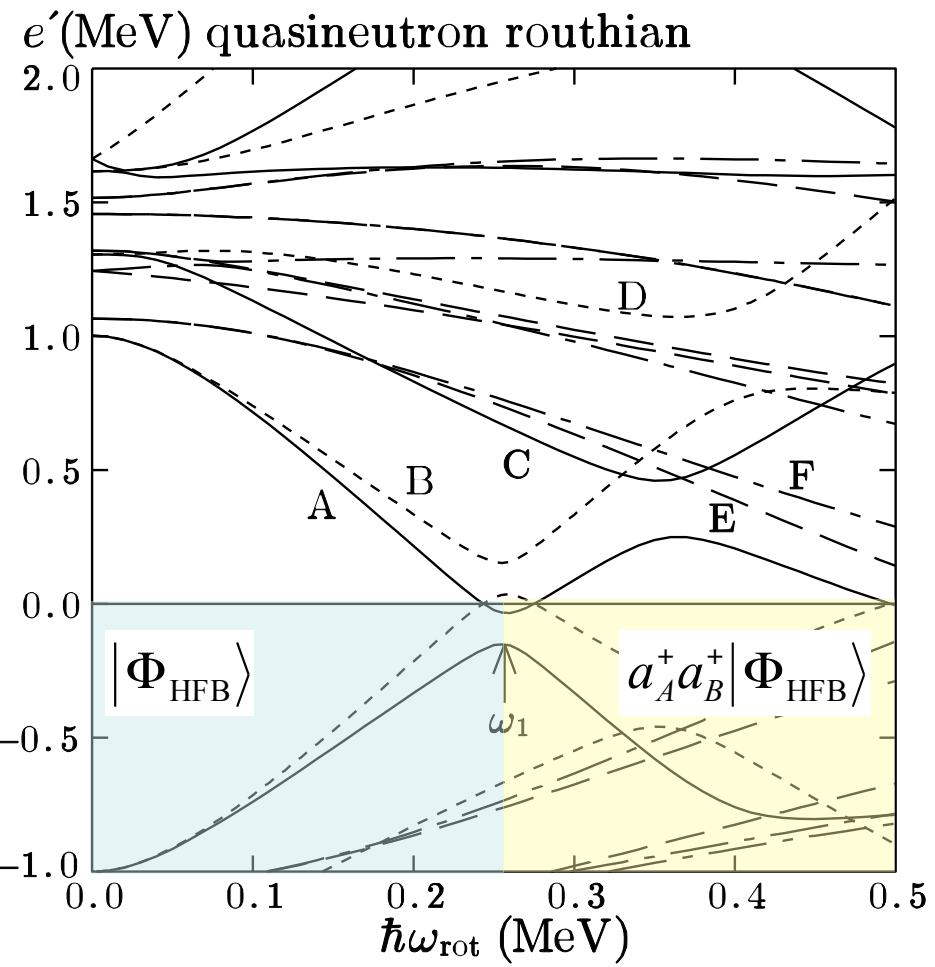
At frequency ω_c , one of the Cooper pair is broken up, due to the Coriolis anti-pairing effect.



$a_A^+ a_B^+ |\Phi_{\text{HFB}}\rangle$

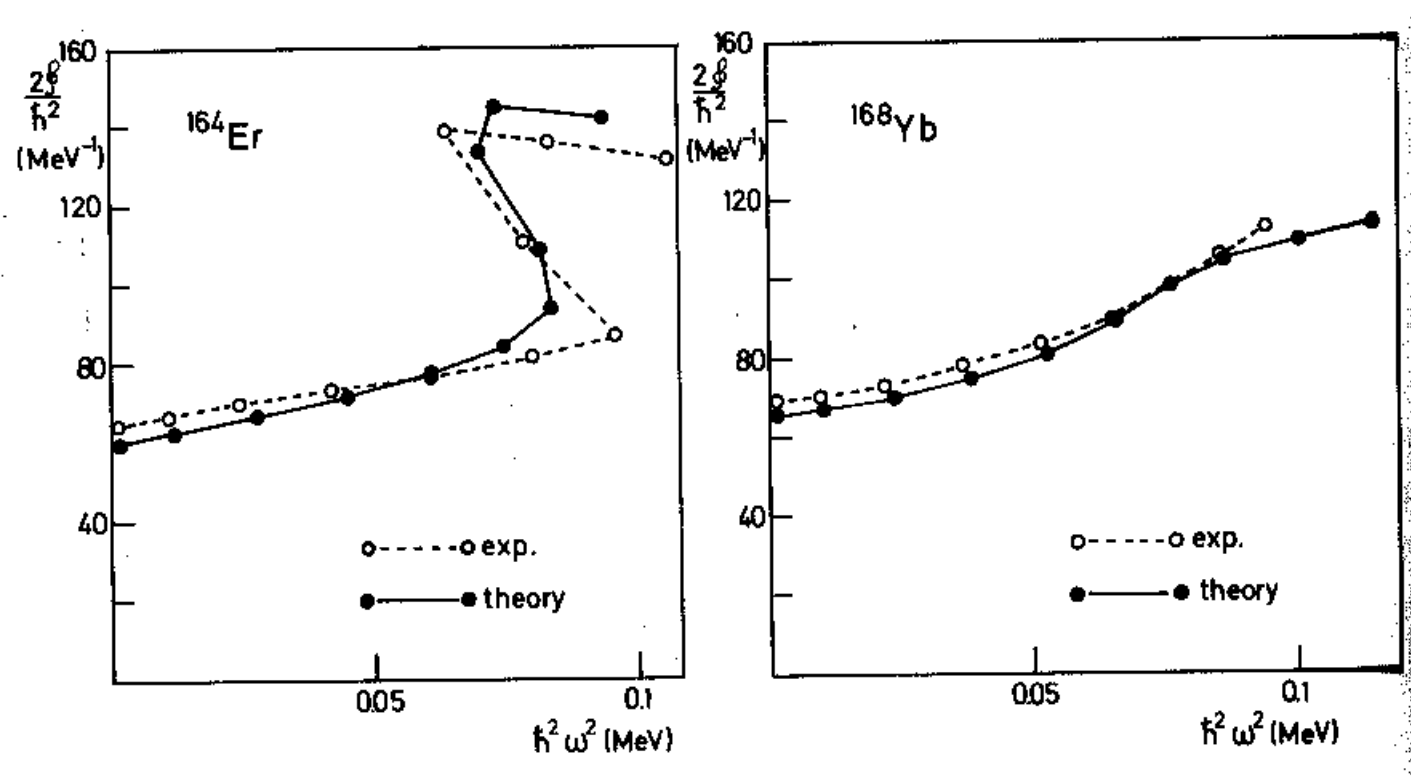


Without increasing ω_{rot} , the state gains about 10 units of spin values, by the alignment.



Cranked HFB model

The cranking model successfully describes the back-bending phenomena in many nuclei, with the proper strength of the Coriolis force.



Systematic analysis

Systematic analysis of the back-bending frequency (by Garrett)

$$\omega_c^{\text{exp}} \approx \frac{1.67\Delta}{j_{\max}}$$

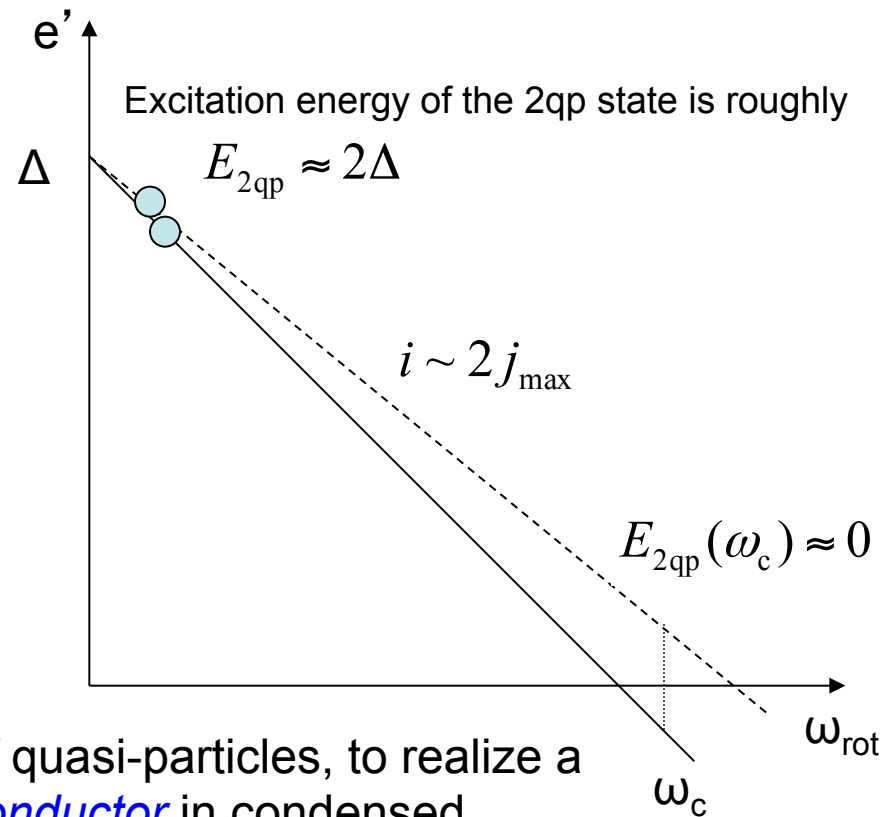
where j_{\max} is the largest j near the Fermi surface.

Simple picture in the right figure predicts

$$\omega_c \approx \frac{\Delta}{j_{\max}}$$

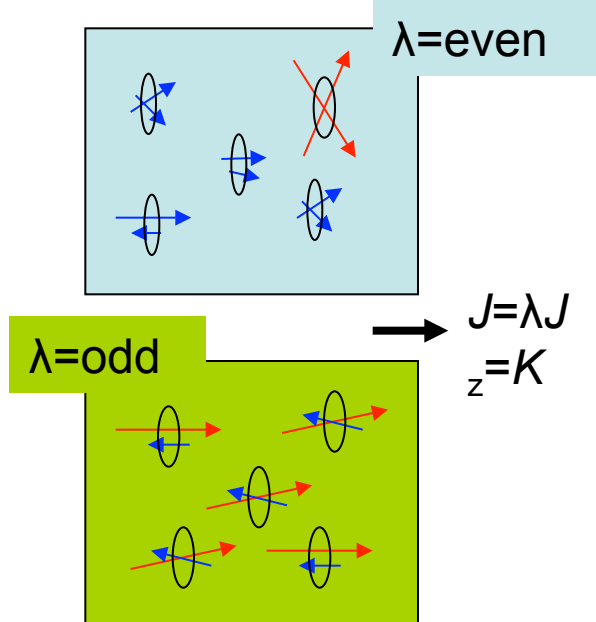
The Coriolis force pulls down the high- j quasi-particles, to realize a state analogous to the *gapless superconductor* in condensed matter.

This can be also regarded as the band crossing between the qp vacuum (0qp) and a 2qp state; **g-band** and **s-band**.



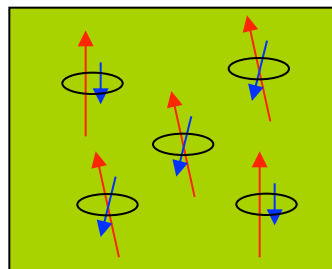
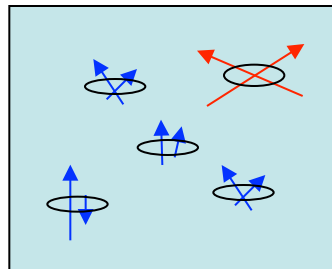
Collective states under rapid rotation

At low spin, many p-h pairs of spin λ contribute to the collective state.



$$|\Phi_{\text{coll}}\rangle \approx \left(\sum_{ph} \alpha_{ph} (c_p^+ c_h)_{\lambda K} \right) |\Phi_0\rangle$$

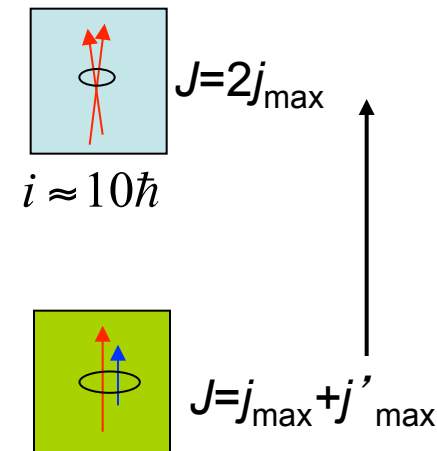
At high spin, each p-h pair is aligned by the Coriolis force, to produce an aligned phonon.



$J = \lambda$
 $J_z = \lambda$

↑

At even higher spin, one of the p-h pairs is completely aligned, by escaping from the λ -coupling.

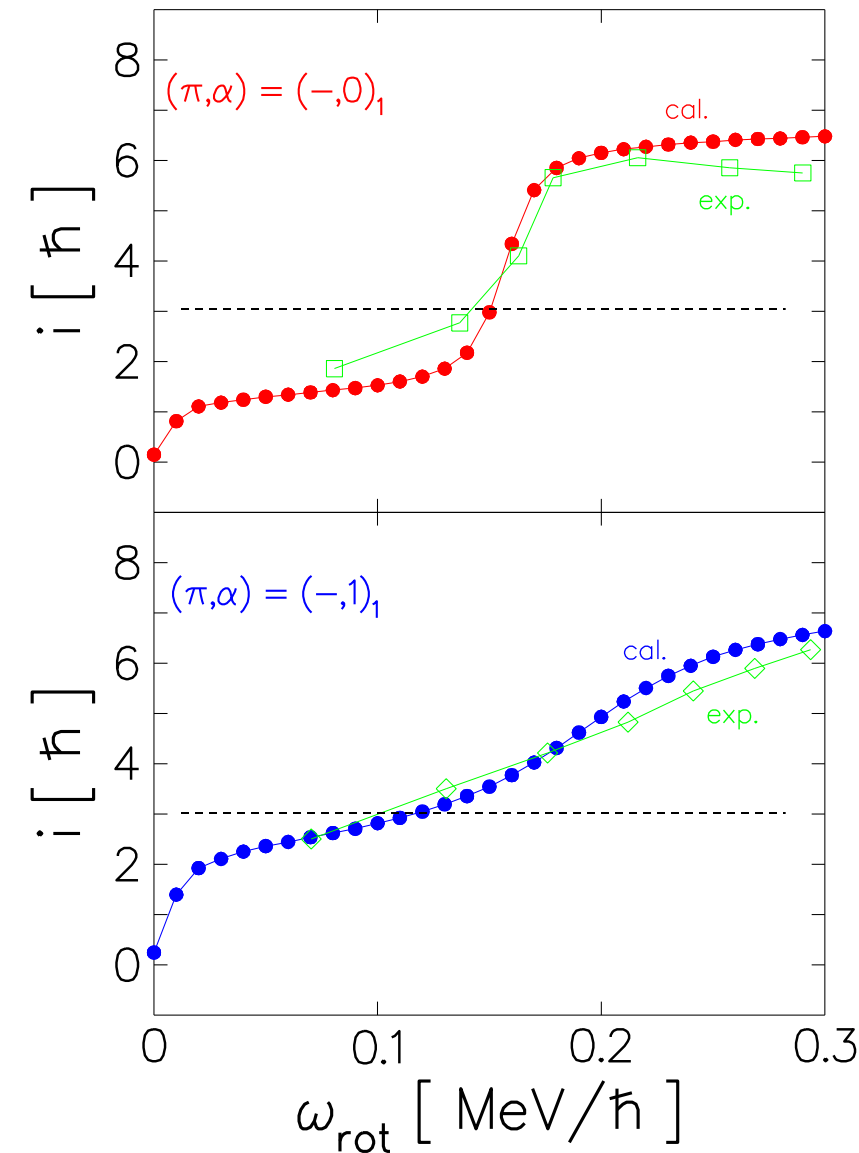
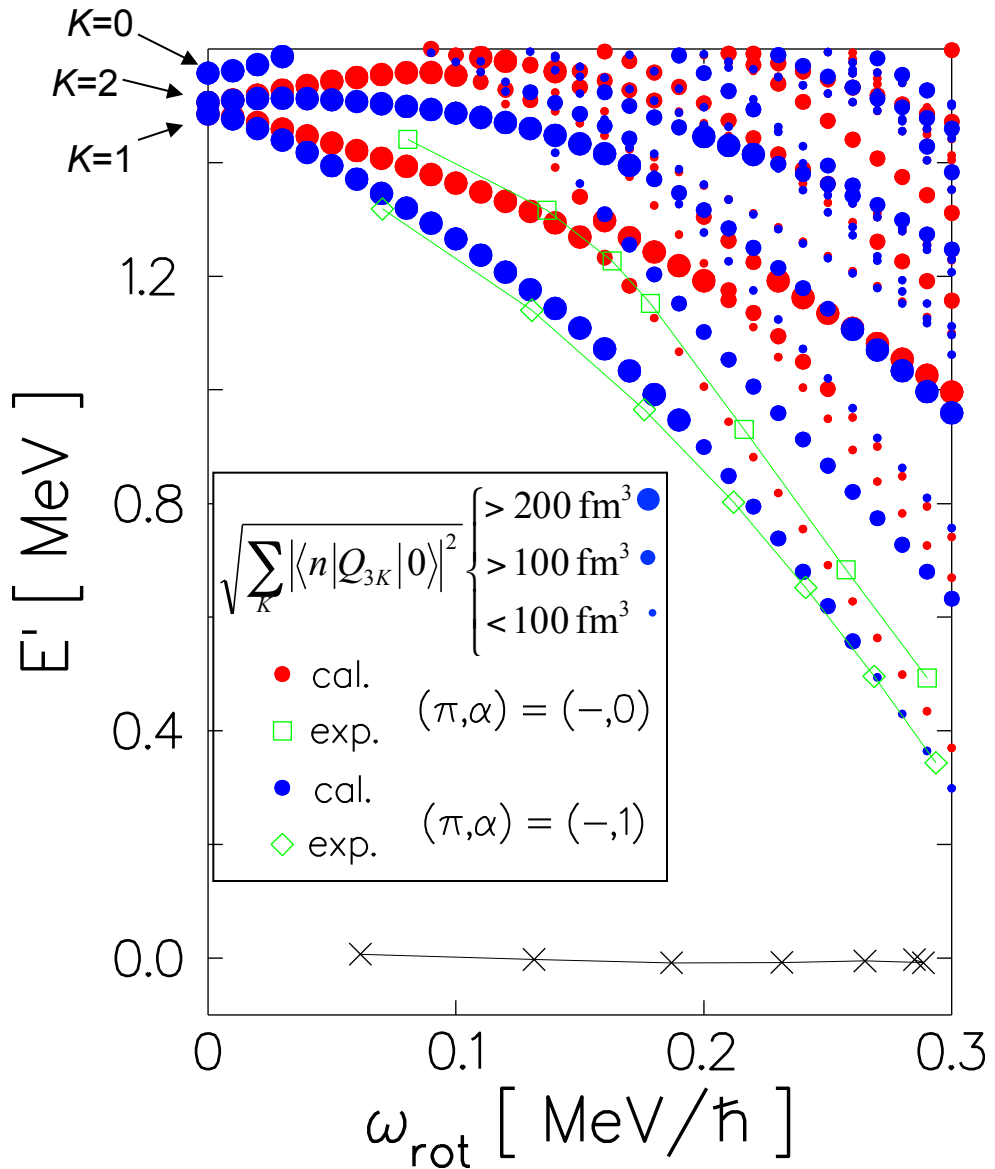


$$|\Phi_{\text{coll}}^{\text{aligned}}\rangle \approx \left(\sum_{ph} \alpha_{ph} (c_p^+ c_h)_{\lambda \lambda} \right) |\Phi_0\rangle$$

$$a_A^+ a_B^+ |\Phi_{\text{HFB}}\rangle$$

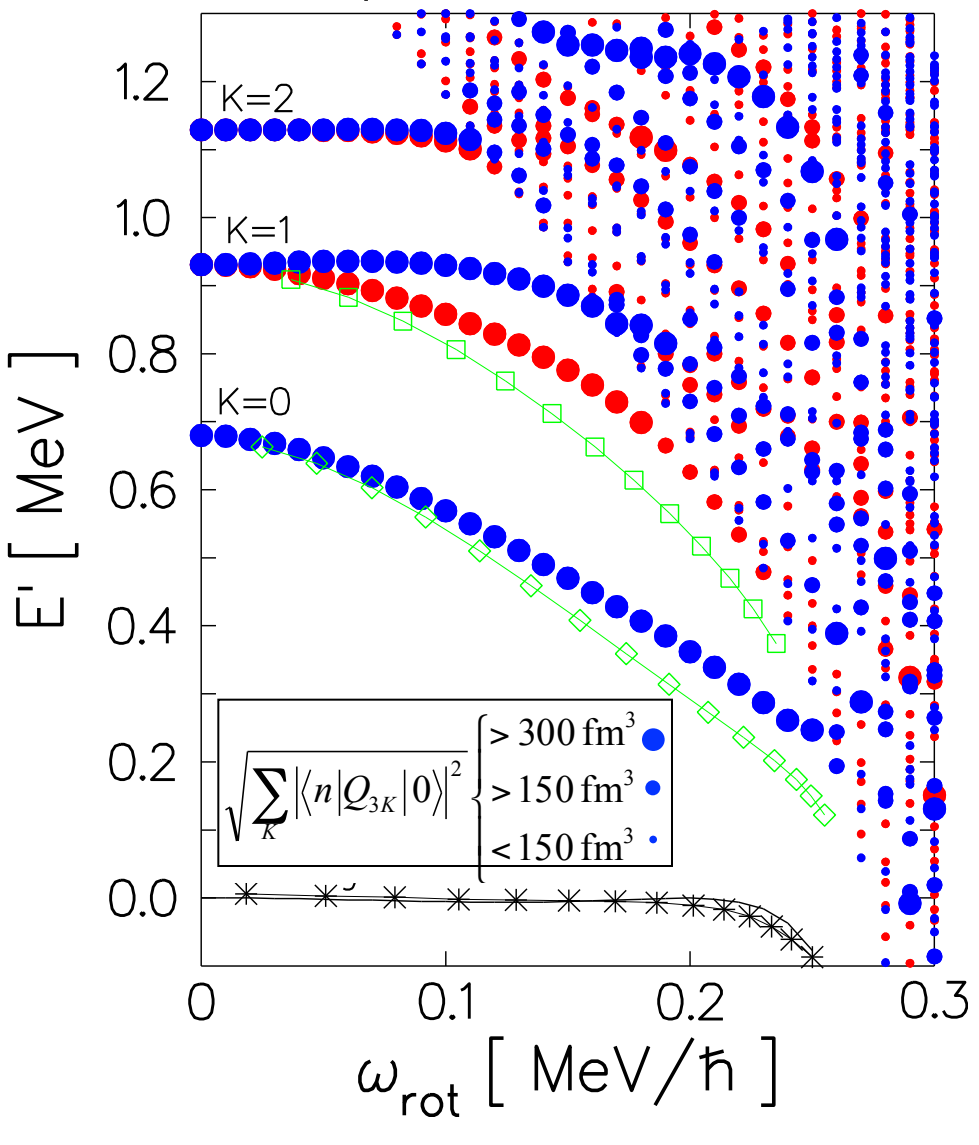
Octupole vibrations in ^{164}Yb

T.N., Act. Phys. Pol. B27 (1996) 59

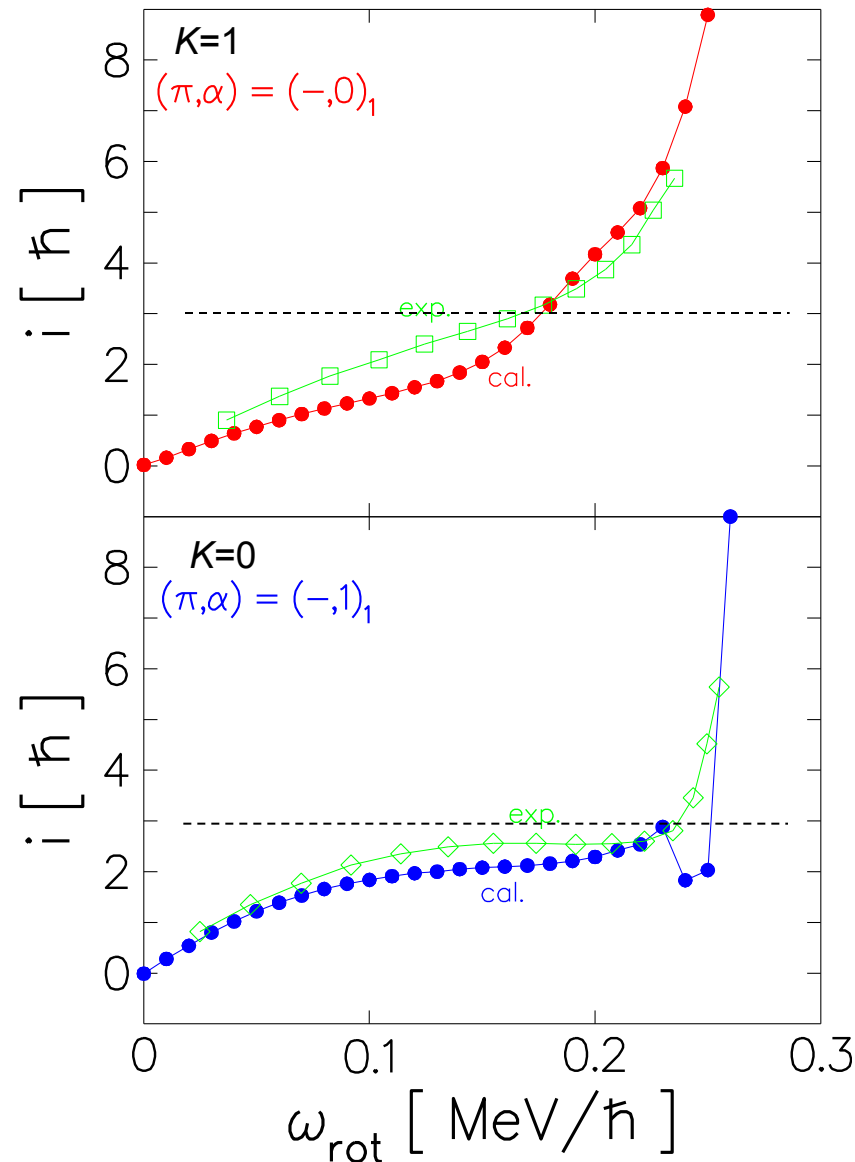


Octupole vibrations in ^{238}U

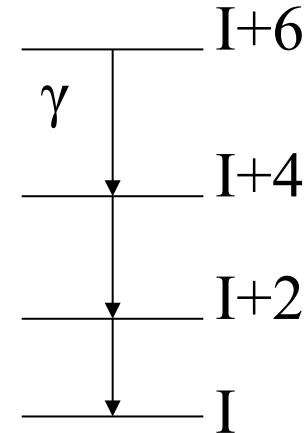
Octupole states in ^{238}U



T.N., Act. Phys. Pol. B27 (1996) 59



In 1986, the first superdeformed band was discovered in ^{152}Dy .



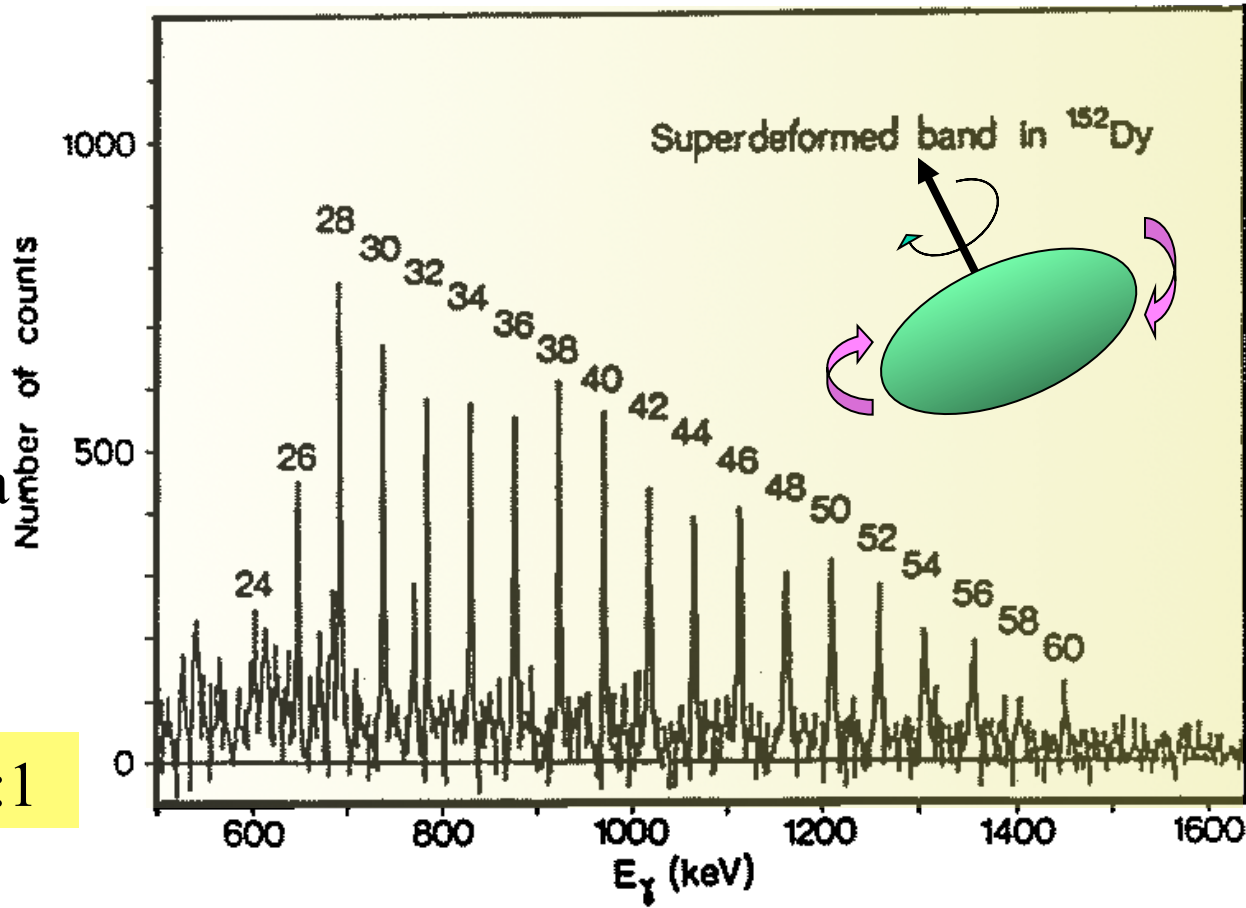
1986 @Daresbury, UK

P.J. Twin et al, PRL 57
(1986) 811

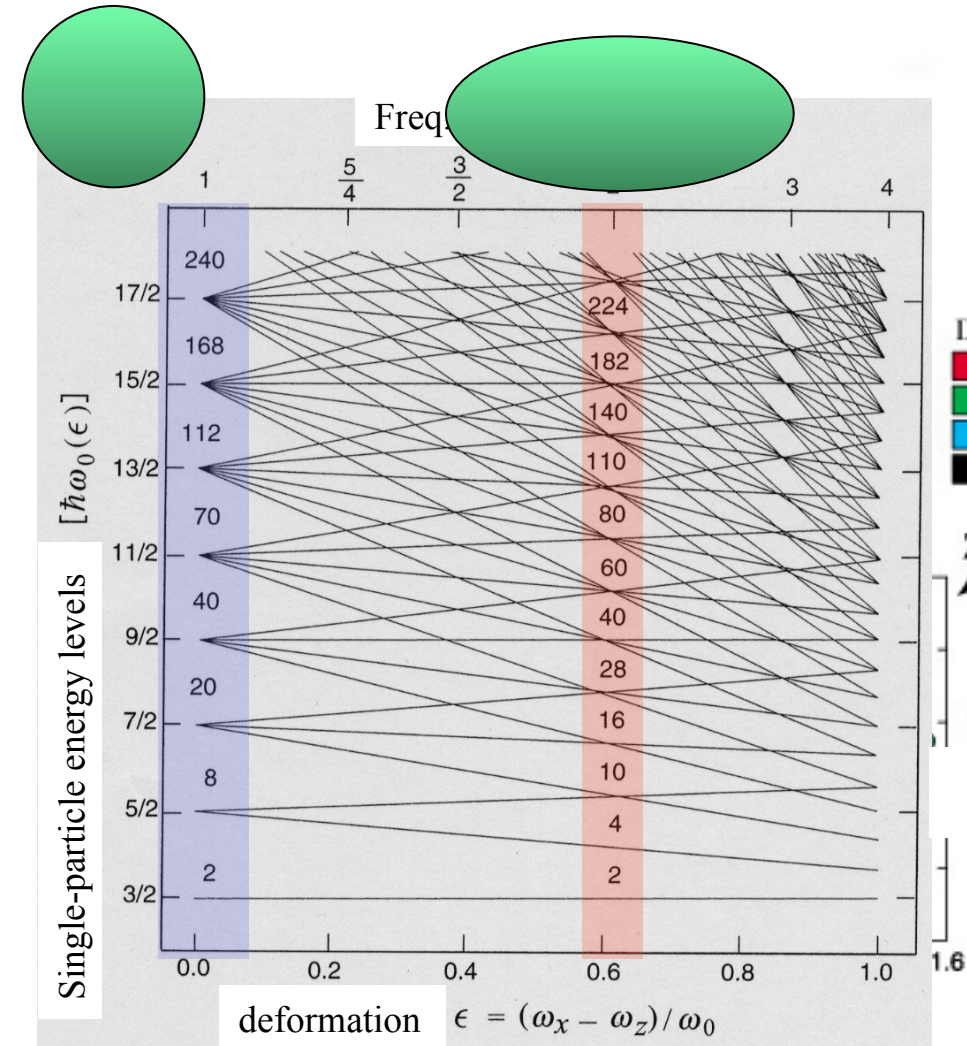
J.D. Garret et al, Nature 323
(1986) 395.

- Large moment of inertia
- Large intraband $B(E2)$
 $B(E2) \approx 2000$ W.u.

Major : Minor axes $\sim 2:1$

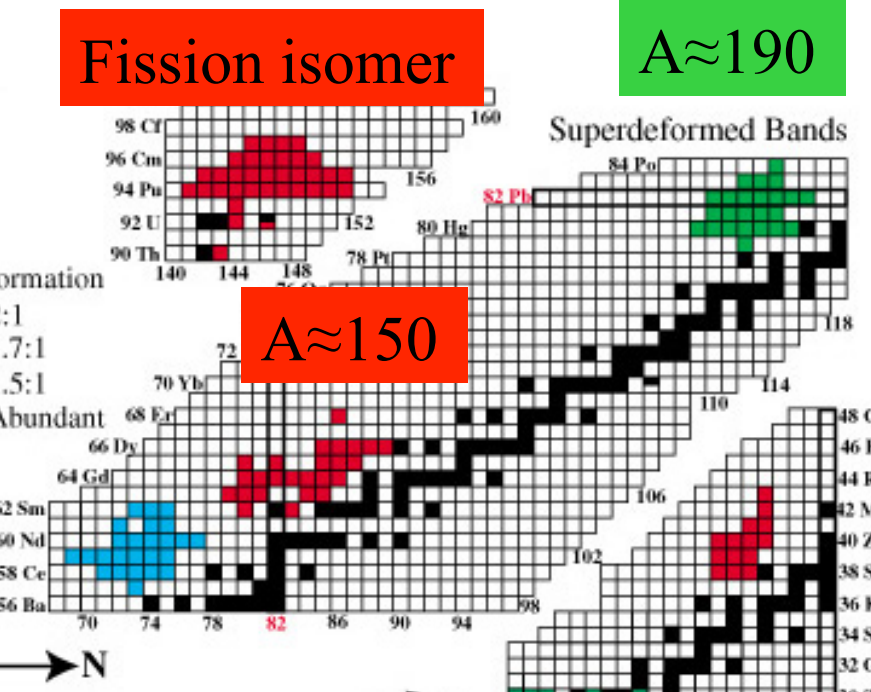


超変形状態は“大変形閉殻配位”



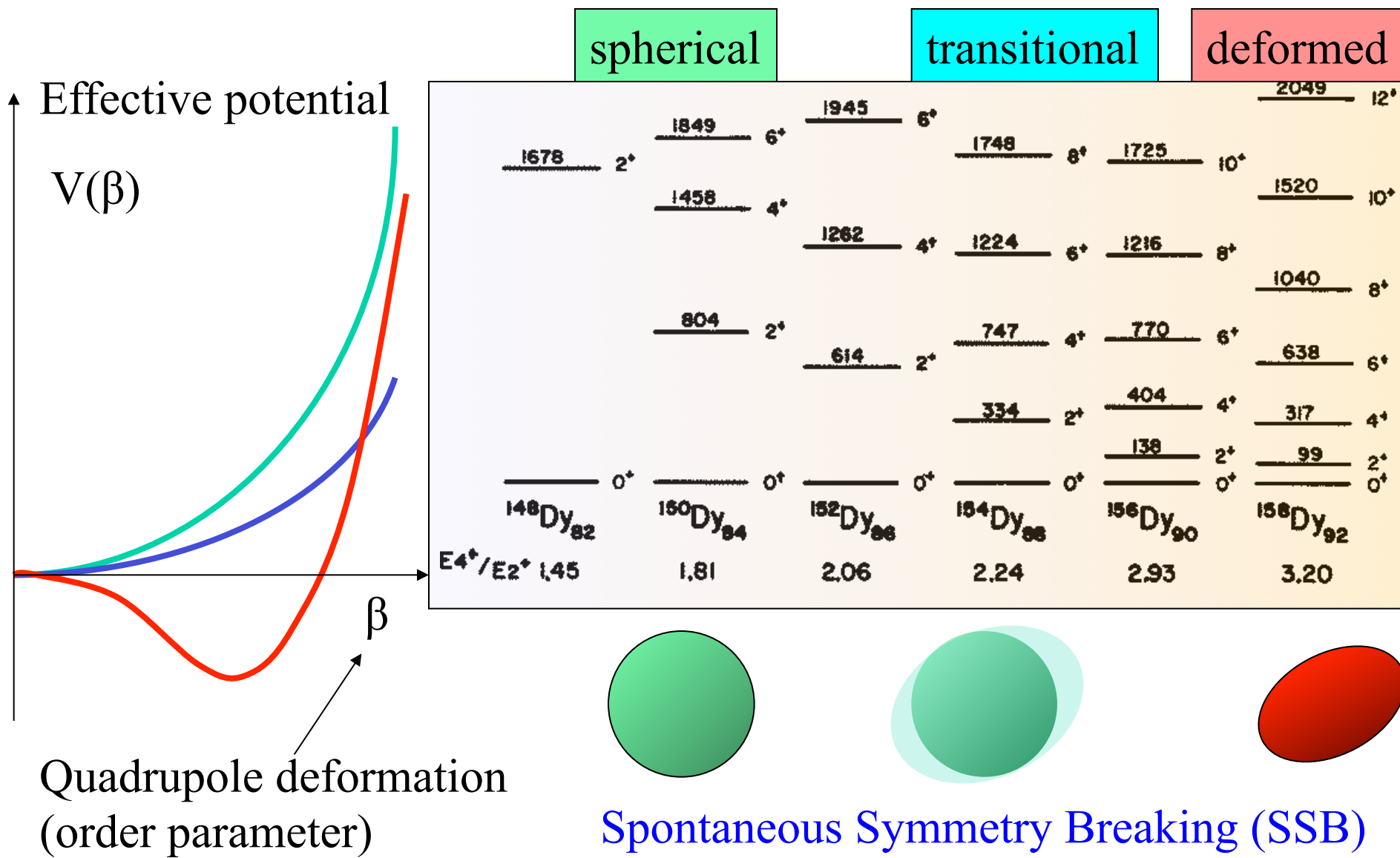
Fission isomer

$A \approx 190$



閉殻 → 閉殻へ

形状相転移(球形閉殻 → 閉殻)



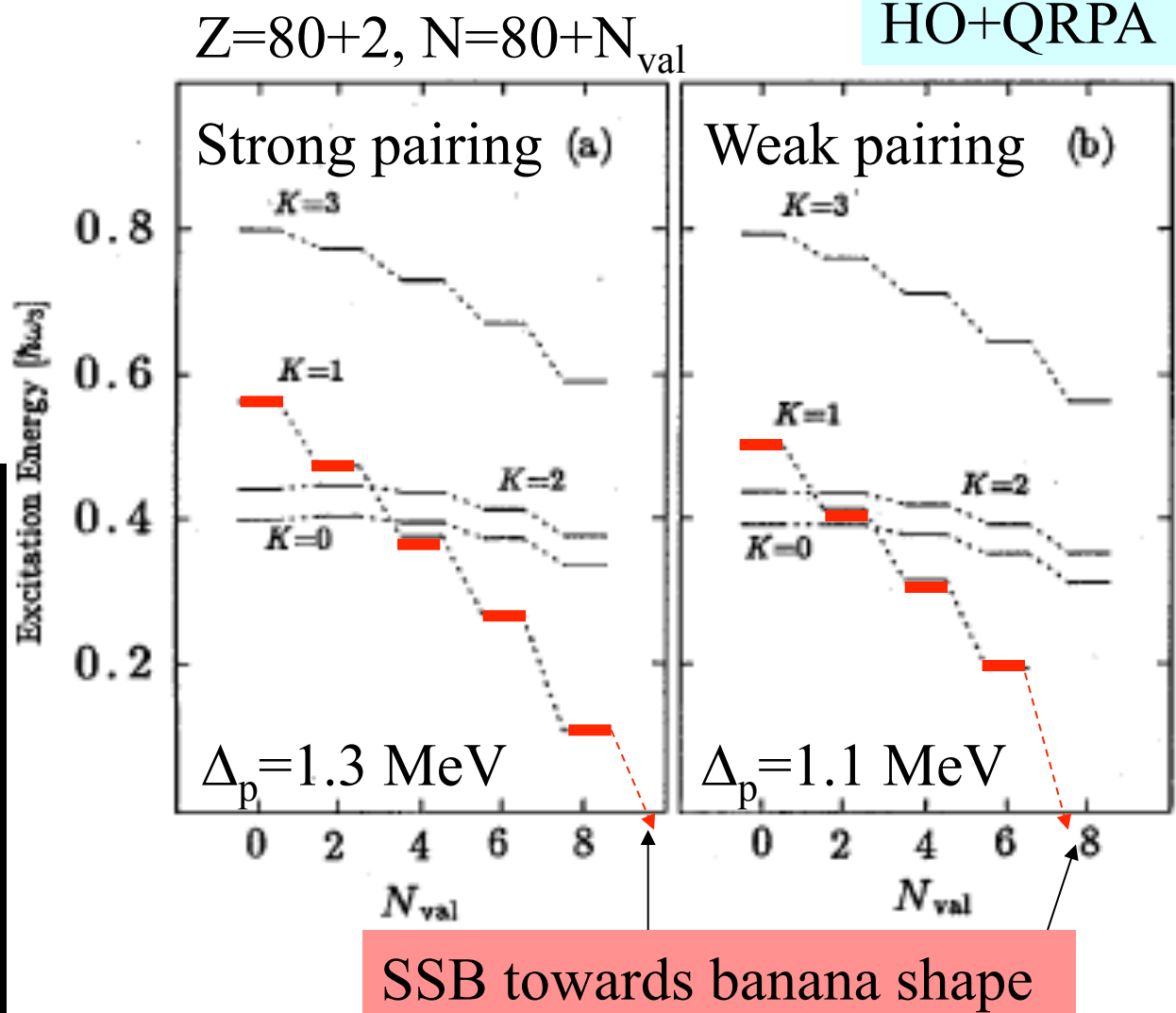
Banana-(Y_{31} -type) shape phase transition in open-shell SD states

T.N., S.M., K.M., Prog. Theor. Phys. **87** (1992) 607.

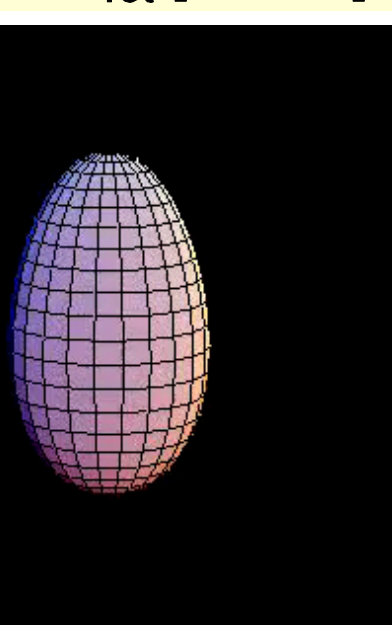
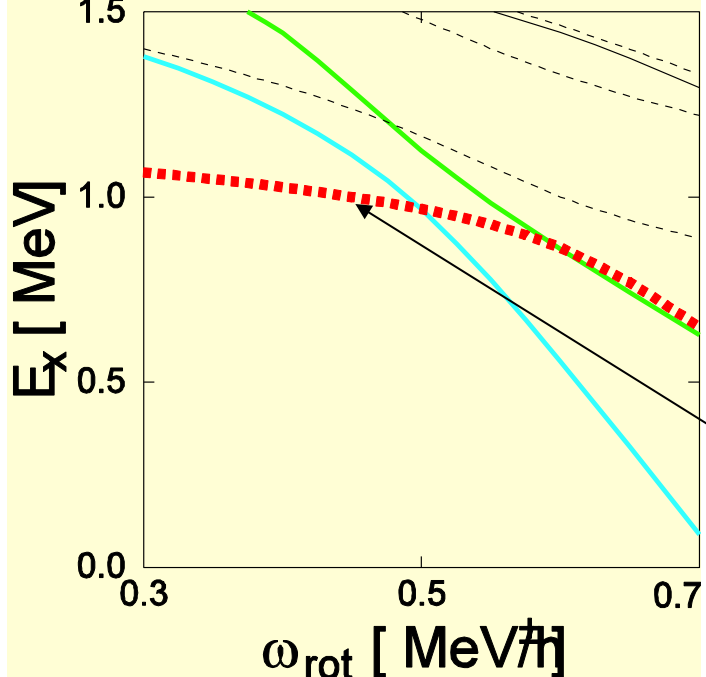
Increase of valence nucleons



Banana-super-deformation



RPA routhians for SD ^{152}Dy

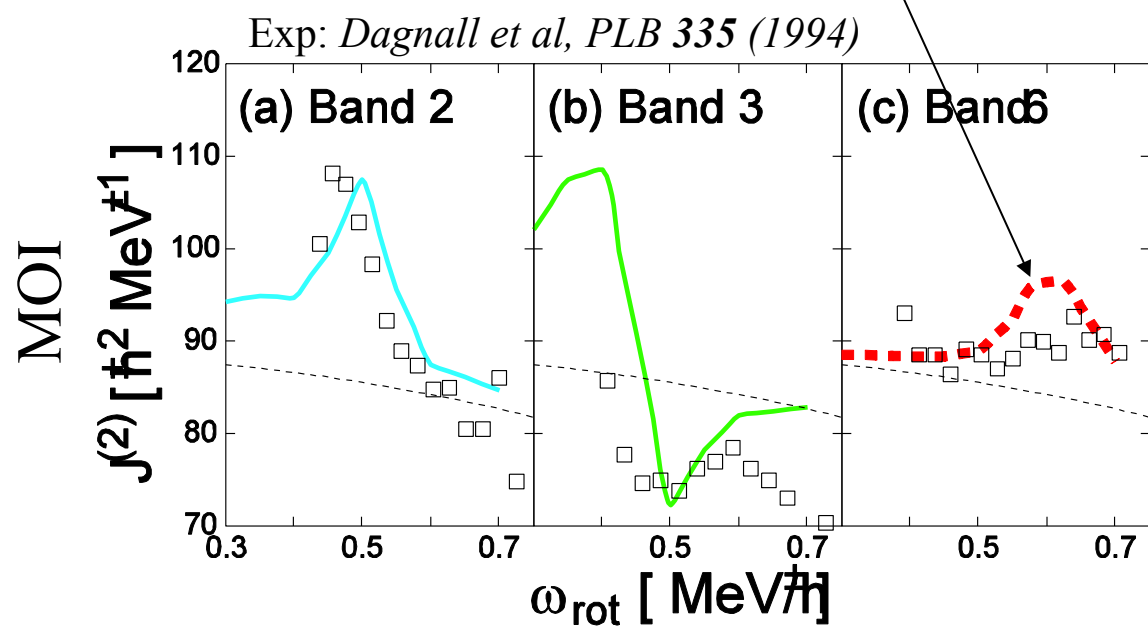


Excitation energy in the rotating frame relative to the ground-state SD band.

RPA in the rotating shell model predicted an excited SD band in ^{152}Dy is the $K=0$ octupole vibrational band.

T.N., Mizutori, Matsuyanagi, Nazarewicz, PLB343 (1995) 19

Octupole band with $K=0$ (Y_{30})



Octupole Vibration in Superdeformed $^{152}_{\text{66}}\text{Dy}_{\text{86}}$

T. Lauritsen,¹ R. V. F. Janssens,¹ M. P. Carpenter,¹ P. Fallon,² B. Herskind,³ D. G. Jenkins,¹ T. L. Khoo,¹ F. G. Kondev,¹ A. Lopez-Martens,⁴ A. O. Macchiavelli,² D. Ward,² K. Abu Saleem,¹ I. Ahmad,¹ R. M. Clark,² M. Cromaz,² T. Døssing,³ A. M. Heinz,¹ A. Korchik,⁴ G. Lane,² C. J. Lister,¹ and D. Seweryniak¹

¹Argonne National Laboratory, Argonne, Illinois 60439

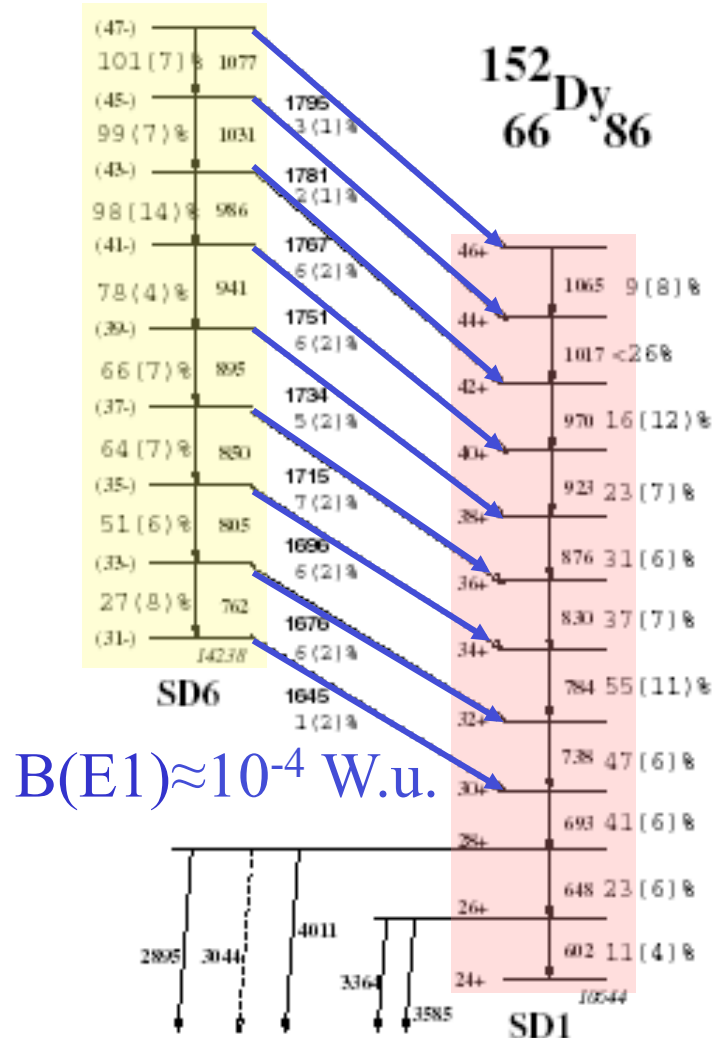
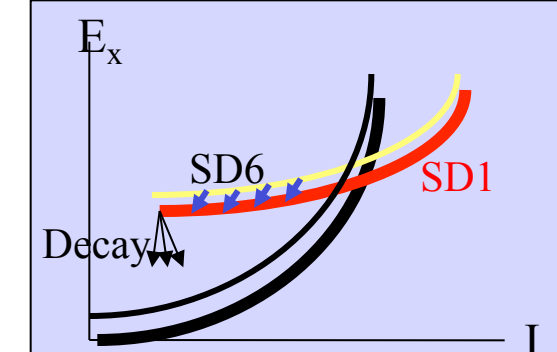
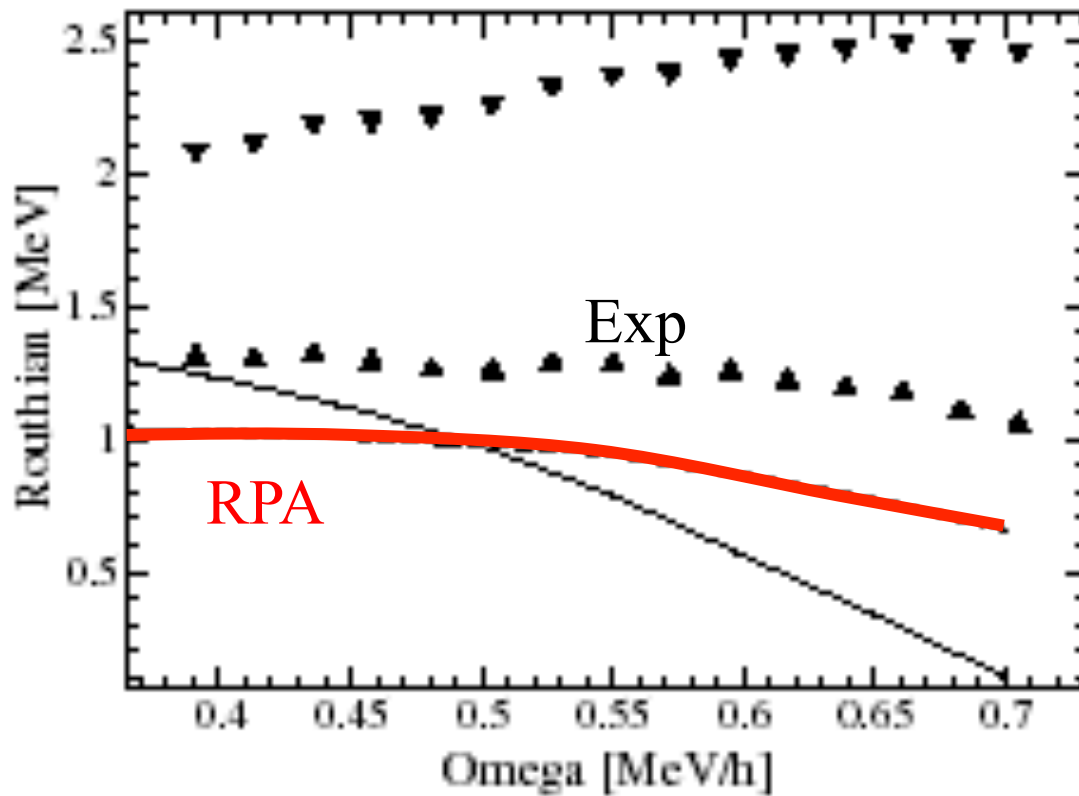
²Lawrence Berkeley National Laboratory, Berkeley, California 94720

³Niels Bohr Institute, DK-2100, Copenhagen, Denmark

⁴C.S.N.S.M., IN2P3-CNRS, bat 104-I08, F-91405 Orsay Campus, France

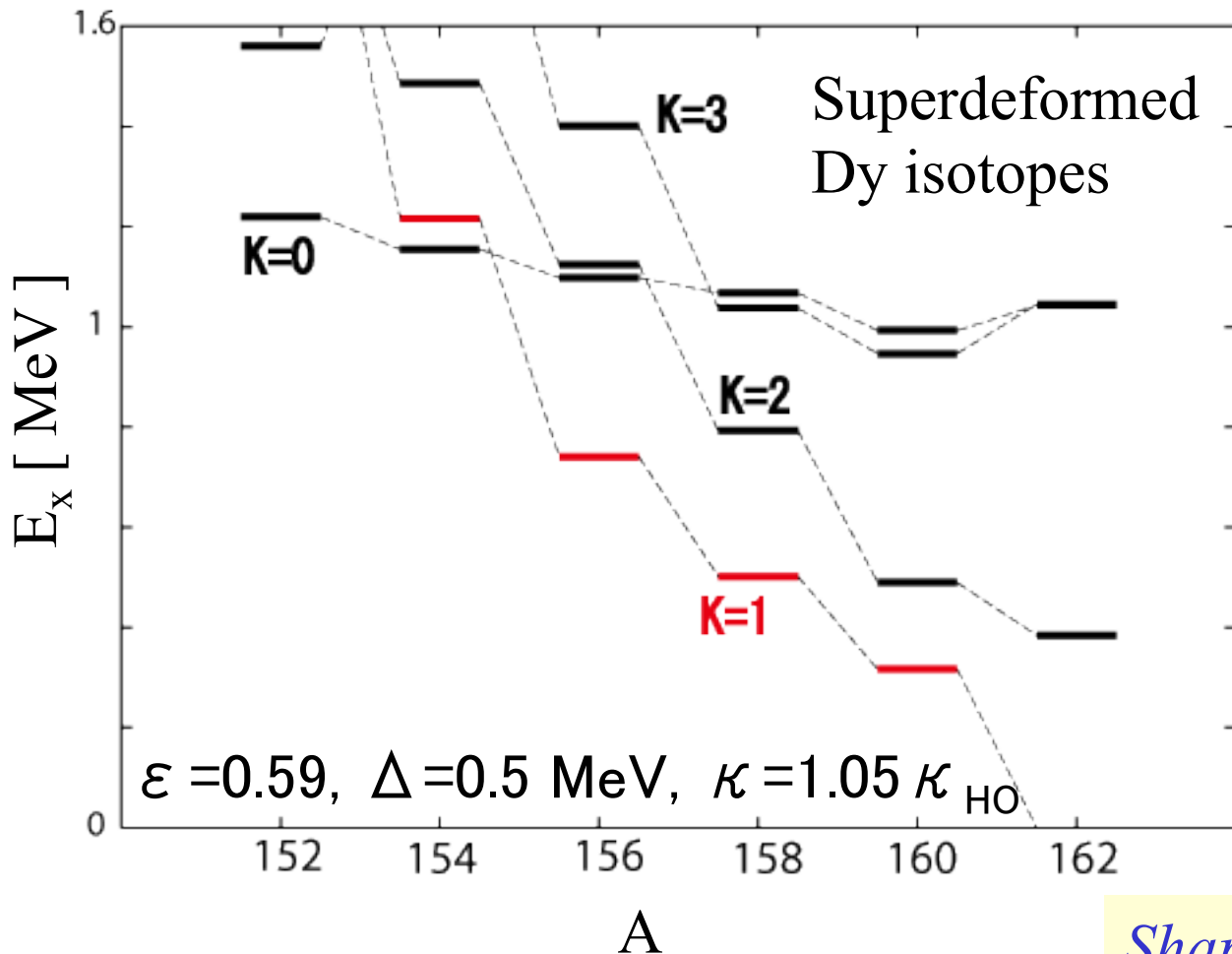
(Received 7 June 2002; published 31 December 2002)

Nine transitions of dipole character have been identified linking an excited superdeformed (SD) band in ^{152}Dy to the yrast SD band. As a result, the excitation energy of the lowest level in the excited SD band has been measured to be 14 238 keV. This corresponds to a 1.3 MeV excitation above the SD ground state. The levels in this band have tentatively been determined to be of negative parity and odd spin. The measured properties are consistent with an interpretation in terms of a rotational band built on a collective octupole vibration.



More realistic calculation

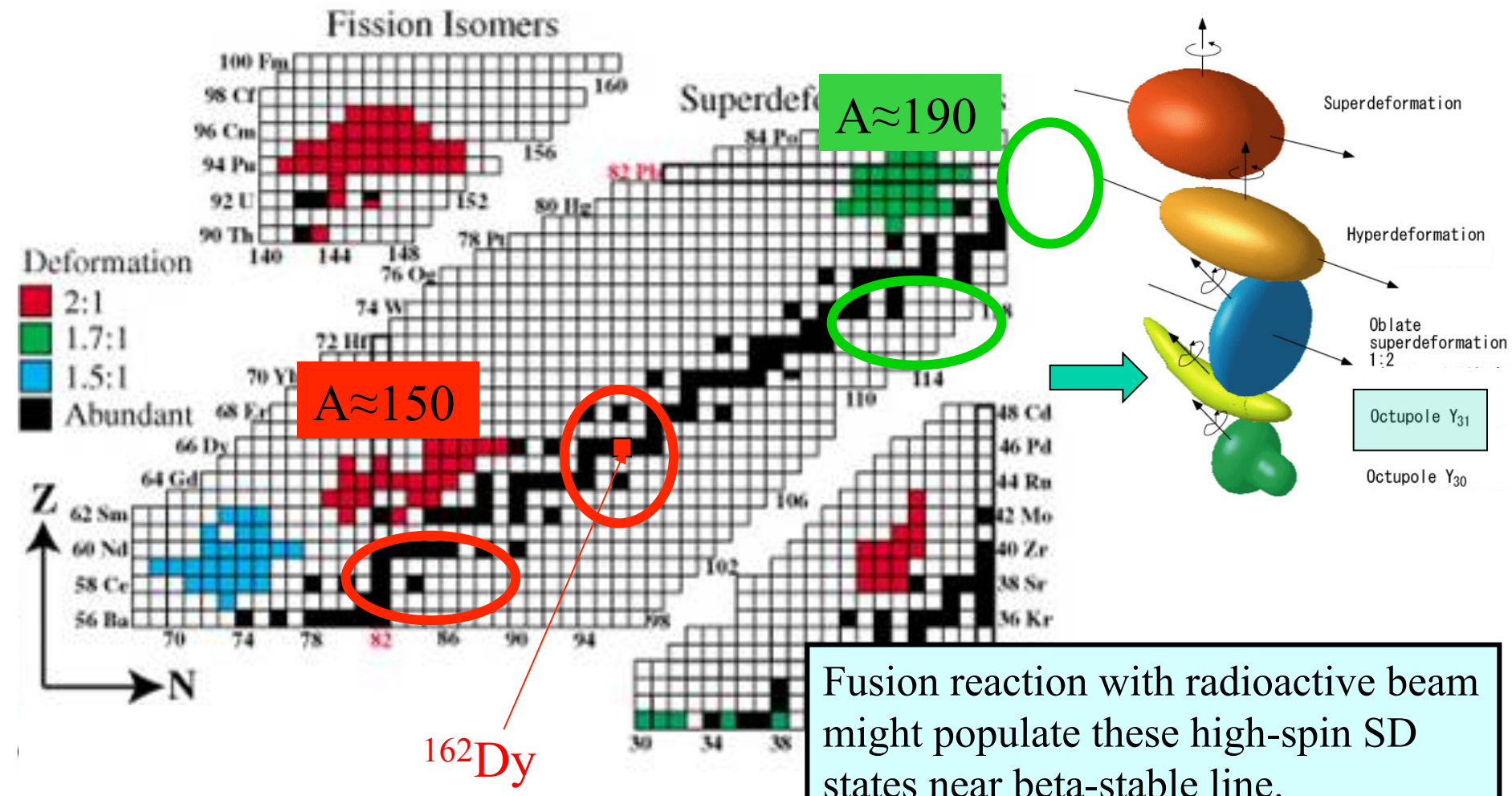
Nilsson+BCS+QRPA



*Shape transition to
banana-super-deformation*

Where are they?

Increasing (decreasing) valence neutrons (protons) by 8-10 leads to regions near beta-stable line



まとめ

- 原子核の性質
 - 強い量子性、フェルミ多体系
 - 異なる時間スケールと異なる描像
 - 有限の相関時間における対称性の自発的破れ
- 高速回転・超変形と形状相転移
 - 回転運動の出現
 - 強いコリオリ相関による様々な現象
 - 超変形閉殻・開殻配位における形状相転移